CHEMISTRY
A EUROPEAN JOURNAL

DOI: 10.1002/chem.200601244

# A Comparative Relativistic DFT and Ab Initio Study on the Structure and Thermodynamics of the Oxofluorides of Uranium(IV), (V) and (VI)

**Grigory A. Shamov, Georg Schreckenbach,* and Thach N. Vo[a]**

**Abstract:** All the possible uranium(VI, V, IV) oxides, fluorides and oxofluorides were studied theoretically by using density functional theory (DFT) in the generalised gradient approximation (GGA), and three different relativistic methods (all-electron scalar four component Dyall RESC method (AE), relativistic small-core ECPs, and zeroth order regular approximation ZORA). In order to test different correlation methods, for the two former relativistic methods hybrid DFT, and, for the AE method, MP2 molecular orbital calculations were performed as well. Single-point AE-CCSD(T) energies were calculated on MP2 geometries as well. Energies of the uranium(VI) and (V) oxofluorides dissociation, uranium(VI) fluoride hydrolysis and oxofluoride disproportionation were calculated and compared against the available experimental thermochemical data. AE-CCSD(T) energies were the closest to the experiment. For GGA DFT methods, all the relativistic methods used yield similar results. For thermochemistry, the best quantitative agreement with the experimental and CCSD(T) values for both U=O and U−F bond strengths was obtained with hybrid DFT methods, provided that a reliable basis set was used. Both the GGA DFT and MP2 MO methods show overbinding of these bonds; moreover, this overbinding was found to be not uniform but strongly dependent on the coordination environment of the uranium atom in each case. U=O vibrational frequencies given by hybrid DFT, however, are systematically overestimated, and are better reproduced by GGA DFT; MP2 values usually fall in-between. Reaction enthalpies, U=O frequencies and complex geometries given by the PBE, MPBE, BPBE, BLYP and OLYP GGA functionals are quite similar, with OLYP performing slightly better than the others but still not as good as hybrid DFT. The geometries of the molecules are found to be influenced by the following factors: the inverse transinfluence (ITI) of the oxygen ligand and, for $U^{V}$, and $U^{IV}$, the Jahn–Teller distortion.

**Keywords:** ab initio calculations · density functional calculations · fluorides · relativity · uranium

## Introduction

Theoretical ab initio quantum chemical and density functional (DFT) methods have proven to be a very helpful tool for main group and transition-metal compounds.[1] They could also be capable of improving our understanding of the various aspects of the chemistry of the f elements, especially actinides where experiments are often costly and dangerous. However, actinides are difficult objects to study by theoretical methods because of the importance of both relativistic effects and correlation effects for their compounds.[2–4] Since actinide atoms are "big" in terms of computational costs, the computational methods have to be very robust to model systems of chemical interest, yet accurate enough to give sensible results.

The accuracy of the DFT calculations can be tested by comparing the available experimental data against calculated values; comparative studies with other, namely wave-function-based methods are also of great interest. For the actinides, various types of experimental data exist: the most abundant are geometries of the classical Werner-type complexes from X-ray crystal and EXAFS solution spectroscopy and actinyl group stretching frequencies from IR/Raman spectroscopy. However, for such ionic compounds, the selection of a realistic computational model system is difficult,

[a] Dr. G. A. Shamov, Prof. G. Schreckenbach, T. N. Vo
Department of Chemistry, University of Manitoba
Winnipeg, Manitoba, R3T2N2 (Canada)
Fax: (+1) 204-474-7608
E-mail: schrecke@cc.umanitoba.ca

Supporting information for this article is available on the WWW under http://www.chemeurj.org/ or from the author: Table S1 containing the dimensions of the orbital and density basis sets used in AE calculations; Table S2 containing U=O vibrational frequencies calculated by different GGA functionals with the AE relativistic method; description of the complete basis set extrapolation procedure applied for MP2 calculations; Table S3 containing MP2 correlation and total energies of the molecules; these energies were used in the complete basis set extrapolation procedure.

and an accurate treatment of solvent effects is required. (We have addressed some of these issues in our previous paper[5].)

The gas-phase thermochemical data for small actinide molecules, which are of the greatest interest since molecular quantum-chemical calculations mainly refer to the gas-phase, are rather scarce. Unfortunately, for the small molecules for which the gas-phase thermodynamic data are available from mass-spectrometric measurements, generally no geometry (especially bond lengths) information is available. (Moreover, due to the absence of geometrical data for small actinide molecules, in estimating thermodynamical functions researchers often rely on analogies with similar compounds of d elements.) Evidence derived from IR spectra of the molecules trapped in a solid noble-gas matrix can sometimes give an idea about the configuration of molecule.[6] One should notice, though, that the matrix has been shown to have non-negligible influence.[7] However incomplete, the gas-phase data allow separating out environmental effects and concentrating on the testing of model chemistries: relativistic and correlation effects. A number of measurements on the halogenides and oxohalogenides of uranium have been done by Hildenbrandt and co-workers[8–12] and Gorokhov et al.[13] They determined heats of formation as well as bond dissociation energies for $UF_6$, $UF_5$, $UO_2F_2$, $UOF_4$. Ebbinghaus et al.[14] recently reviewed gas-phase standard heats of formation of $UO_3$. For many of these molecules there is also IR and/or Raman spectroscopy data available (in a solid noble-gas matrix; see references [15] and [16] and references therein).

## Previous Theoretical Work

Theoretical studies on uranyl hexafluoride are abundant because of the high symmetry and therefore relative simplicity of the molecule (see ref. [17] and [18] and references therein). Batista et al.[19] investigated the lower uranium fluorides, $UF_5$ and $UF_4$,[18] in their benchmark study of the $UF_n$ bond dissociation energies (BDE). They employed a variety of relativistic methods (small and large core effective core potentials (ECP) as well as an all-electron two-component third order Douglas–Kroll–Hess Hamiltonian (DK3)[20,21]), and density functionals (LDA, GGA and hybrid functionals). It was shown that small core ECPs give results that are in agreement with those of all-electron DK3 calculations while large-core ECPs give wrong results. It was proposed that the reason for this failure is the wrong radial structure (i.e., the absence of nodes in the outer d and s orbitals in case of the large-core ECPs). Hybrid functionals (PBE0 and B3LYP) gave good agreement with the experiment, while GGAs predicted too high values for the BDE. Spin-orbit effects on the BDE were calculated and found to be about $-4\ \mathrm{kcal\,mol^{-1}}$. (This is due to the stabilisation of the dissociation product $UF_5$ which has one unpaired f electron.)

Calculations on the oxides and oxofluorides are rare compared with actinide halogenides. Wang and Pitzer[22] calculated the ground and excited states of $UO_2F_2$; for the ground state, the LDA geometry has been used. The molecule was of $C_{2v}$ symmetry, with an F-U-F angle of 109.6°, and an O=U=O angle slightly distorted from linearity, as 169.5°.

Pyykkö et al.[23] in their paper on high-valent actinide molecules studied, among others, $UO_2F_2$, $PuO_2F_2$, $PuF_6$ and $PuOF_4$. They employed B3LYP and MP2 optimised geometries and small-core ECPs[24] for the actinide atoms. The F-U-F angles for $UO_2F_2$ were found to be 114 and 112°, respectively, by these methods. Apparently, high symmetry has been assumed for the calculations, so they report $PuF_6$ belonging to the $O_h$ and $PuOF_4$ to the $C_{4v}$ point groups. They conclude that for the $f^0$ species both MP2 and B3LYP methods are "reliable and comparable, except in cases with very small HOMO–LUMO gaps". Based on their calculations of the oxofluorides and anionic complexes of uranyl and neptunyl, these authors note that the equatorial bonding to fluorides is of partial 5f $\phi$ character. The latter observation is in agreement with a recent experimental X-ray photoelectron and X-ray emission study on $UO_2F_2$, which showed that in the complex filled 5f orbitals exist, that is, participate in the bonding.[25] Clavaguera-Sarrio et al. in their comprehensive DFT study on $UO_2L_2$-type complexes[26] studied dioxodifluorouranium and found the $C_{2v}$ structure as well.

Uranium trioxide was calculated at the Hartree–Fock (HF) level using LC-ECPs by Pyykkö et al.[27] They found a T-shaped geometry with the odd oxygen-to-uranium bond being longer than for the uranyl oxygens, and a valence angle in uranyl of 161°.

Privalov et al.[28] have used the hybrid density functional B3LYP to study the hydrolysis reactions of $UF_6$ to $UO_2F_2$, and $UO_3$ to $UO_2(OH)_2$. Moreover, they have investigated conproportionation reactions involving the three former molecules. Ab initio calculations, MP2 and CCSD(T), were also performed, based on the SCF-optimised geometries. Small-core Stuttgart-Dresden ECPs[24] were used for uranium. Both the B3LYP and HF methods predicted a bent $C_{2v}$ structure for $UO_2F_2$, with the F-U-F angle of 113.6 and 120.7°, respectively. The $UO_3$ molecule was found to be of distorted T-shaped configuration with the biggest O=U=O angle of 165.2° at the HF level of theory. For the CCSD(T) method, agreement within the experimental uncertainty was achieved for the reaction energies; B3LYP and MP2 gave slightly bigger errors. In the hydrolysis processes larger errors were due to bad treatment of the hydrogen fluoride molecule, one of the hydrolysis products. After removal of these errors by calibration to another reaction (formation of HF from simple compounds), the quality of the results improved considerably. In a subsequent paper, these authors extended[29] the scope of their work to the corresponding complexes of neptunium and plutonium as well. Again, SCF-optimised geometries were used for subsequent energy calculations at the MP2 and CCSD(T) levels of theory. For the plutonium compounds all-electron Douglas–Kroll relativistic calculations were performed, along with minimal active space multi-configurational SCF. Spin-orbit effects

  

were estimated for the Np and Pu compounds. For the actinyl oxide-fluoride conproportionation reaction these were found to be −2.5 and 4.1 kcal mol$^{-1}$, respectively.

All-electron ZORA-DFT calculations on $UF_6$ and $UO_2F_2$ (along with other halides) were performed by Kovacs and Konings.[30] They used a number of GGA density functionals (choosing BP86 as the best one) in the optimisation of geometries. F-U-F and O=U=O angles in $UO_2F_2$ were found to be 110.6 and 168.0°, respectively. Both of these angles decrease substantially for the complexes of the other halogens, in the row F > Cl > Br > I. This trend was explained in terms of increasing covalent and decreasing ionic character of the metal−halogen bonding along the series.

To our knowledge, the only theoretical work to date performed on $UOF_4$ (as well as the other uranium monooxo tetrahalogenides) was the very recently published paper by Kovacs and Konings.[31] They used primarily the MP2 method along with small-core ECPs for uranium, as well as GGA and hybrid DFT methods with ZORA and the same small-core ECPs correspondingly. They found that the ECP-based MP2 and hybrid DFT predict $UOF_4$ to have a trigonal-bipyramidal $C_{3v}$ configuration, while all-electron GGA DFT predicted a $C_s$ structure close to a tetragonal pyramid with oxygen in one of basal positions. For the latter, the authors have noted that the potential energy curve for bending of the F-U-F angle from the $C_s$ to the $C_{3v}$ configuration was very shallow. They considered the geometries given by MP2 and hydrid DFT as the most reliable ones, and explained the stereochemistry of the monoxauranium tetrahalogenides in the scope of the inverse-*trans*-influence (ITI) concept.

The results cited above show that, in general, spin-orbit effects have indeed some influence on the thermodynamics, but it is limited to a few (about 4–5) kcal mol$^{-1}$. The experimental error bars and/or divergences between different experimental results for the gas-phase thermochemical parameters of the actinides (which mostly come from mass spectrometry) are comparable to or even larger than that value. Moreover, other sources of errors we have in our computational methods (for example, approximations for the correlation energy) are larger compared with the neglect of the spin-orbit effects. For that reason, it is worthwhile to apply approximate DFT methods using some scalar-relativistic approach, even without spin-orbit interactions and multiplet effects. Literature results for the actinide triatomics[32] comparing DFT calculations with multi-configurational spin-orbit ones are encouraging.

The actual choice of DFT method is also of interest. In their recent paper, Moskaleva et al.[33] successfully predicted the heat of formation of gaseous $UO_2^{2+}$ based on the enthalpies of a set of isodesmic reactions involving $UF_6$ and $UO_2^{2+}$ with some other small organic molecules. Moskaleva et al. used GGA DFT with an all-electron relativistic Douglas–Kroll[20,21] method. Batista et al.[19] pointed out that hybrid DFT gives the best agreement with the experiment as compared to GGA for the $UF_6$ bond dissociation energies. For the vibrational spectra of $UF_6$ and $UF_5$, hybrid DFT also gave better agreement than GGA. However, it was found[34,35] that GGA give better vibrational frequencies for actinyl stretches; and that hybrids might underestimate the covalency for the uranium(III) and lanthanide compounds. Comparison for the aqueous redox potentials of actinyl aqua complexes, as well as hydration energies of bare actinyls did not show significant preferences for hybrids over GGAs, while actinyl frequencies were again closer to the experimental ones for the latter.[5] Therefore, it is important to know whether not only uranium−halogen bonds are described better by hybrid DFT, but multiple uranium-to-oxygen bonds as well. We have to note that GGA DFT methods are much cheaper in terms of computational cost than hybrid DFT, and therefore the usage of the former might be unavoidable for larger actinyl-containing systems, which makes the comparative study of GGA performance actual and practically important.

**Scope of the current work—model reactions**: In this work, we will use a number of small molecules, namely fluorides, oxides and oxofluorides of uranium for which there are experimental thermochemical data available, to test the performance of GGA and hybrid DFT functionals with relativistic methods that are practically affordable for the treatment of "real" systems of chemical interest. Moreover, we will try to compare the most affordable wavefunction-based correlation method, second-order Møller–Plesset many-body perturbation theory (MP2). It is well known that wavefunction-based correlated methods converge much slower than DFT with respect to the basis set. In order to have meaningful comparison of the MP2 method with the GGA and hybrid DFT methods, we will gradually increase the size of the basis set used, and employ the complete basis set extrapolation (CBS) technique.[36] Finally, to determine the importance of the higher-order correlation corrections, we will use single reference coupled cluster energies (albeit only as single-point calculation using MP2 geometries, for the obvious practical reasons).

As the model test system, we will use bond strengths for all the possible fluorides, oxides and oxofluorides of uranium(VI) with the general formula $UF_{(6-2n)}O_n$; $n = 0$–3. We will calculate the corresponding homolytical bond dissociation energies (BDE) directly, as well as consider processes in which the energies of U−F and U=O bonds are included implicitly, as for oxide-fluoride conproportionation reactions and fluoride hydrolysis. Previously, the BDEs of the uranium halogenides were calculated by Batista et al.[19] and $UF_6$ hydrolysis reactions were studied already by Privalov et al.[28] Here we will consider both of these test systems with the same set of methods, and include all of the oxofluorides into consideration. This will allow us to go beyond the BDEs of halogenides, and to also include strengths of U−F bonds next to U=O bonds as well as the U=O bond dissociation. Moreover, we will see if the strengths of these bonds depend on the environment of the uranium atom.

To calculate the (homolytic) BDEs for the complexes of uranium(VI), we will need all its low-valence products. In this study, we will limit it up to an oxidation degree of four

  

(which corresponds to removal of one oxygen or two fluorine atoms from the $UF_{(6-2n)}O_n$ molecule). Therefore, the ten species with the following oxidation states have to be considered:

VI $UF_6$, $UOF_4$, $UO_2F_2$, $UO_3$

V $UF_5$, $UOF_3$, $UO_2F$

IV $UF_4$, $UOF_2$, $UO_2$

Using the energies calculated for these species, a number of reaction energies could be calculated and compared to the available experimental and earlier theoretical data. First we will consider conproportionation reactions between oxides and fluorides of uranium(VI). The energy of reaction (1) was calculated already by Privalov et al.[28] One can construct reactions (2) and (3) in order to include $UOF_4$. For this molecule, the standard heat of formation is also available, but the corresponding bond energies, to the best of our knowledge, have not been calculated to date:

$$UF_6 + 2\,UO_3 \rightarrow 3\,UO_2F_2 \quad (1)$$

$$UF_6 + UO_2F_2 \rightarrow 2\,UOF_4 \quad (2)$$

$$UOF_4 + UO_3 \rightarrow 2\,UO_2F_2 \quad (3)$$

The following dissociation processes are of interest (because there are some experimental data available, at least for the uranium case considered here):

$$UF_6 \rightarrow UF_5 + F \quad (4)$$

$$UF_5 \rightarrow UF_4 + F \quad (5)$$

$$UOF_4 \rightarrow UOF_3 + F \quad (6)$$

$$UOF_4 \rightarrow UOF_2 + 2\,F \quad (7)$$

$$UOF_4 \rightarrow UF_4 + O \quad (8)$$

$$UO_2F_2 \rightarrow UO_2F + F \quad (9)$$

$$UO_2F_2 \rightarrow UO_2 + 2\,F \quad (10)$$

$$UO_2F_2 \rightarrow UOF_2 + O \quad (11)$$

$$UO_3 \rightarrow UO_2 + O \quad (12)$$

Another possible class of processes comprises hydrolysis reactions of $UF_6$:

$$UF_6 + H_2O \rightarrow UOF_4 + 2\,HF \quad (13)$$

$$UF_6 + 2\,H_2O \rightarrow UO_2F_2 + 4\,HF \quad (14)$$

$$UF_6 + 3\,H_2O \rightarrow UO_3 + 6\,HF \quad (15)$$

Of course, many other processes could be considered (such as conproportionations of uranium(V) and (IV) oxides and fluorides, hydrolysis of uranium(V) and (IV) fluorides,. However, we restricted the scope of our paper to processes for which we were able to compare our results with experimental thermochemical data. Moreover, the selected test reaction set allows for testing U−F and U=O bond energies both directly, as in the homolytic dissociations (4)–(12), and relative to each other, as in (1)–(3) and (13)–(15).

The structure of the present paper is as follows. First, we will describe the details of the calculations in the Computational Methods section. Then, geometries and electronic structure of all the uranium molecules under study (see above) will be discussed. After that we will compare experimental and calculated U=O vibrational frequencies and, finally, the enthalpies of the reactions (1)–(15).

## Computational Methods

As noted in the previous section, many earlier studies used some assumptions about the symmetry of the uranium complexes. Also, in many cases the approach of calculating single-point final energies on geometries obtained by a lower level of theory was used. This might be a source of errors. In this work, unless noted otherwise, we fully optimize geometries of the molecules without any symmetry constraints, and calculate energies on the geometries optimised by the same method. For that reason, all the relativistic/correlation methods and codes we chose had to be capable of effective analytical calculation of at least first derivatives of the energy. For all the optimised structures of our complexes (unless otherwise noted), harmonic vibrational frequencies were calculated with the same program and basis sets to verify the nature of the stationary points obtained. They were also used for the calculation of the thermal contributions to the reaction enthalpies.

For systems with odd number of electrons, the unrestricted Kohn–Sham (or Hartree–Fock in case of wavefunction methods) method was used. All the species of uranium(IV) were considered as triplets.

We will apply three different relativistic schemes: an all-electron scalar four-component method with the relativistic spin-orbit effects separated out and neglected (AE), relativistic effective core potentials (ECP), and the zeroth-order regular approximation (ZORA). Where possible, we will use several correlation methods for each relativistic method: for all three relativistic methods, we will use GGA density functionals, and for the two former we will also use hybrid DFT. For the AE method we use second-order Møller–Plesset perturbation theory[37] (MP2) as the most affordable wavefunction-based alternative to DFT. Details of the complete basis set (CBS) extrapolation scheme are provided in the Supporting Information.[36]

Also, single-point single-reference coupled cluster calculations including singles, double and perturbative triple configurations (CCSD(T)[36,38]) using the AE relativistic method and the L1 basis sets were performed on the MP2/L3 optimised geometries. In these calculations, we used MP2/L2 frequencies for the thermochemistry, just as for the MP2/CBS case.

**Relativistic methods**: All-electron, scalar relativistic calculations were performed using the Priroda code,[39–41] version 5.04. All-electron scalar-relativistic (AE) DFT and MP2 calculations are performed using the spin-free Hamiltonian derived by Dyall.[42] Atomic basis sets of generally-contracted Gaussian functions are used to expand the electronic wavefunctions and to approximate the product densities for calculating the two-electron terms of DFT and MP2. The wavefunction basis sets of correlation-consistent type[43] are atomically-balanced contractions of kinetically-balanced primitive functions. The density basis sets are generated[44] to accurately represent occupied–occupied and occupied–virtual products

  

of atomic wavefunctions. The dimensions of the wavefunction and density basis sets (the number of radial functions for angular momenta l = 0, 1, etc.) are presented in the Supporting Information, Table S1, where the notation L1, L2, L3 is used for the double, triple and quadruple set sizes. Note that the large L3 basis set goes up to *g* functions on O and F and *i* functions at U, respectively, (*h* and *m* functions, respectively, for the accompanying density basis sets).

The scalar-relativistic DFT implementation is based on the approximate evaluation of Coulomb[45] and GGA exchange-correlation[39] terms using density fitting with the Coulomb metric. This allows for an even larger improvement in computational speed compared with the non-relativistic case. First and second derivatives of the energy with respect to nuclear coordinates are computed analytically. The scalar-relativistic MP2 implementation[41] uses the resolution-of-identity approximation of the two-electron integrals calculating both the HF and the correlation energies, the analytic first derivatives with respect to nuclear coordinates are available. Also we note that for all AE calculations very fine integration grids and tight ($10^{-5}$) optimisation convergence criteria were used throughout this work.

Most of the AE-DFT calculations were performed in the L1 basis set. In order to test basis set effects on the thermochemistry, the L2 bases from the same work were used for some AE-GGA calculations as well. All AE-MP2 geometry optimisations and frequency calculations were performed both in the L1 and L2 basis sets. Moreover, geometries were optimised within the L3 basis sets as well (although no frequency analysis was performed) which allowed for applying a complete basis set extrapolation scheme[36] for MP2 energies of the molecules studied. In all AE-MP2 calculations, the first ($30n+m$), (where $n$ is the number of uranium atoms, and $m$ the number of fluorine or oxygen atoms in the molecule) molecular orbitals were frozen.

The zeroth-order regular approximation (ZORA)[46–48] for relativistic effects was used as implemented in the ADF[49–51] program package. The standard all-electron ZORA-TZP Slater-type basis sets were employed for all the atoms. Scalar ZORA was applied when we performed the unconstrained optimisations and frequency calculations for all the molecules. An integration criterion of 5.5 was used, and geometries were optimised until the maximum component of the energy gradient became less that $10^{-4}$ a.u.

Relativistic effective core potentials (ECP) calculations were performed using the Gaussian 03 program package.[52] The small-core relativistic core potential (SC-ECP) by Küchle et al.[24] was used for the uranium atom. The corresponding basis set for the uranium (labeled "SDD SC 1997") was taken from the EMSL basis set repository,[53] with the most diffuse s, p, d, and f primitives removed. For the main-group elements, standard 6-31G** basis sets, and in some cases cc-pVTZ[54] basis sets as implemented in the Gaussian 03 package[52] were used. In the latter case, a single *g* polarisation function with the exponent 0.5 was added to the basis set of the uranium atom. We termed these basis set combinations B1 and B2, respectively.

For all three relativistic methods used, we used the Perdew, Burke and Ernzerhof (PBE)[55] exchange and correlation GGA density functional, which demonstrated good overall performance for standard tests.[56] For the AE scalar relativistic method and the SC-ECP method, we also used the hybrid density functional PBE0,[57] containing 25% of the exact exchange. This functional was shown[58] to have good performance for f element compounds.

In order to test the influence of the selection of GGA density functional on the reaction energies, we have done AE scalar relativistic calculation using a range of GGA functionals other than PBE. First, we have tried the recent PBE modification[59] (termed MPBE hereafter). Then, we considered the well-established Becke exchange functional[60] together with the correlation functional by Lee, Yang and Parr (LYP)[61] as well as with PBE correlation functional (abbreviated as BLYP and BPBE, respectively). Finally, we used a combination of Handy's and Cohen's exchange functional[62] with the LYP correlation functional, called OLYP.

For the analysis of the electronic structure of some of the compounds studied, we used Mayer population bond orders[63] and Hirshfeld[64] ("fuzzy-atoms") atomic charges obtained from AE-DFT calculations.

**Selection of the experimental thermodynamic data**: For small molecules such as water or HF, as well as for the simple compounds $O_2$ and $F_2$, well-established gas-phase thermochemical experimental data exist. However, the experimental data published for uranium compounds sometimes diverge more than the experimental error bar allows. We have taken the gas-phase values from the work of Hildenbrand and Lau[9] for the $\Delta H^f_{298}(UF_6) = -513\,kcal\,mol^{-1}$, the revised value of $\Delta H^f_{298}(UF_5) = -461\,kcal\,mol^{-1}$, and $\Delta H^f_{298}(UF_4) = -382\,kcal\,mol^{-1}$. This results in U–F bond dissociation energies (BDE) for $UF_6$ and $UF_5$ of 70.6 and 97.4 kcal $mol^{-1}$, respectively. The gas-phase values of $\Delta H^f_{298}(UO_2F_2) = -323\,kcal\,mol^{-1}$ and $\Delta H^f_{298}(UOF_4) = -414\,kcal\,mol^{-1}$ were taken from earlier work of the same authors.[11] The value of the standard heat of formation of the gaseous $UO_3$ was taken as $-190.5\,kcal\,mol^{-1}$, which is a recommended value from the report of Ebbinghaus et al.;[14] $\Delta H^f_{298}(UO_2) = -111.5\,kcal\,mol^{-1}$ was taken from the paper by Green.[65]

## Results and Discussion

### Structures of molecules

The geometries of water and hydrogen fluoride are well known, and will thus not be discussed any further. Below we will describe the geometries of uranium-containing molecules given by different relativistic and correlation methods. For convenience we will group them by the types of $UX_3$, $UX_4$ and $UX_5$, with the remaining molecules $UF_6$ and $UO_2$ treated separately. The numeration of the atoms is described in Scheme 1. Geometry parameters and point groups of each type are provided in Tables 1–4.

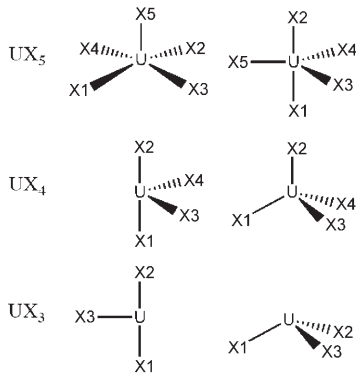


Scheme 1. Numbering scheme for $UX_3$, $UX_4$ and $UX_5$-type molecules presented in Tables 1–5. One of the oxygen atoms in the molecule, if there are any, is always $X_1$.

**$UF_6$ and $UO_2$ (Table 1)**: Results for these two molecules are given in Table 1. For $UF_6$, there are experimental gas phase results available for bond lengths. The closest values to the experimental ones (which are reported to be 1.999(3)[66] or 1.996(8)[67] Å) are given by the hybrid DFT methods. The PBE functional always give longer distances for U–F in $UF_6$ than hybrid DFT. We note that Mayer bond orders[63] for the bonds, calculated by both DFT functionals, are higher than unity (see Table 5 and Discussion section). This is in agreement with previous calculations by Pyykkö et al.[68]

  

who explained the partial multiple bond character in $UF_6$ by π-back-donation from the fluorine atoms to the uranium. The bond orders predicted by hybrid DFT are lower and charges on the atoms are higher than those given by GGA. MP2-optimised bond lengths decrease with increasing basis set size from L1 to L3, yielding shorter bonds than the experimental values for the latter basis.

For the $UO_2$ molecule, all methods predicted a linear configuration. One can see that the U=O bond lengths given by different methods show the same trend: PBE gives longer bonds than the hybrid DFT (Table 1), MP2 bond lengths, although decreasing with increasing the basis, are in-between the two former.

**$UX_3$-type (Table 2)**: First, we consider the uranium trioxide. As usual,[5] pure GGA gives longer uranium-to-ligand bonds than hybrid DFT. AE-DFT calculations, both hybrid PBE0 and pure GGA PBE, predict a slightly distorted planar T-shaped form for the molecule, with a lower *trans*-O=U=O angle for the latter method. SC-ECP DFT calculations give similar results, as do ZORA PBE calculations. The "uranyl" U=O bonds are predicted to be shorter than the "oxide" U=O bond by all DFT methods; however, the latter is considerably shorter than an usual, ordinary uranium–oxygen bond. The population (Mayer) bond orders[63] calculated at the AE-DFT level (Table 5) suggest that all three U=O bonds are of considerable triple-bond character.

The MP2 method, however, gave different results depending on the basis set used. The MP2/L1 calculation yielded a $D_{3h}$ configuration for $UO_3$. However, in the L2 basis set, we found a T-shaped $C_{2v}$ structure instead, which turned out to be a transition state between two Y-shaped $C_{2v}$ minima. The MP2/L3 optimisation converged to a similar Y-shaped structure. We have optimised $UO_3$ also in the SC-ECP MP2 approach using the B1 and B2 basis sets and obtained a trigonal-pyramidal $C_{3v}$ structure in both cases. For the MP2/B1 calculation, U=O distances were found of 1.885 Å and O=U=O angles of 109.2°.

The structure of the uranium trioxide was studied experimentally[16] by isotope-substituted IR spectroscopy in a solid noble-gas matrix and found to be of T-shaped configuration corresponding to a "uranyl-oxide". The extent of the matrix influence is, however, unknown. We have calculated $UO_3$ with the AE-PBE/L1 method with its geometry fixed to a $D_{3h}$ symmetry; the resulting structure (which is not a stationary point) has an energy only 1.75 kcal $mol^{-1}$ above the one of the T-shaped configuration.

The $UO_2F$ geometries calculated by DFT (both pure and hybrid) with the AE and SC-ECP relativistic approaches were found to be T-shaped of $C_{2v}$ symmetry (Table 2). AE-MP2 calculations yield a T-shaped geometry of lower symmetry $C_s$.

For the planar T-shaped $UOF_2$, *cis*- and *trans*-configuration of the fluorides are potentially possible. SC-ECP calculations with the B1 basis set found that the *trans*-isomer is 7.7 and 12.3 kcal $mol^{-1}$ less stable than the *cis*-isomer for PBE and PBE0, respectively. We note that with the larger B2 basis, a PES minimum corresponding to the *trans*-isomer of $UOF_2$ cannot be located. AE-PBE/L1 calculation also didn't find a minimum for the *trans*-isomer, leading to a planar *cis*-isomer of $C_s$ symmetry. Similar results were obtained for

Table 1. Calculated geometries of $UF_6$ and $UO_2$. Bond lengths in angstroms, angles in degrees; see Scheme 1 for numbering (*trans* atoms in parentheses).

| | Parameter | AE | | | | | G03, SC-RECPs | | ADF ZORA |
|---|---|---|---|---|---|---|---|---|---|
| | | PBE/L1 | PBE0/L1 | MP2/L1 | MP2/L2 | MP2/L3 | PBE/B1 | PBE0/B1 | PBE/TZP |
| $UF_6$ | point group | $O_h$ | $O_h$ | $O_h$ | $O_h$ | $O_h$ | $O_h$ | $O_h$ | $O_h$ |
| | $r_{U-X1}$ | 2.024 | 1.997 | 2.005 | 1.993 | 1.990 | 2.015 | 1.990 | 2.025 |
| $UO_2$ | point group | $D_{\infty h}$ | $D_{\infty h}$ | $D_{\infty h}$ | $D_{\infty h}$ | $D_{\infty h}$ | –[a] | $D_{\infty h}$ | –[a] |
| | $r_{U-X1(X2)}$ | 1.815 | 1.784 | 1.814 | 1.805 | 1.802 | –[a] | 1.776 | –[a] |

[a] No convergence.

Table 2. Geometries of the uranium species isomorphous to $UO_3$, calculated by different methods. Bond lengths in angstrom, angles in degrees; see Scheme 1 for numbering (geometry labels in parentheses refer to *trans* atoms); ITI% for a given bond also in parenthesis, see text for details.

| | Parameter | AE | | | | | G03, SC-RECPs | | ADF ZORA |
|---|---|---|---|---|---|---|---|---|---|
| | | PBE/L1 | PBE0/L1 | MP2/L1 | MP2/L2 | MP2/L3 | PBE/B1 | PBE0/B1 | PBE/TZP |
| $UO_3$ | point group | $C_{2v}$ | $C_{2v}$ | $D_{3h}$ | $C_{2v}$ | $C_{2v}$ | $C_{2v}$ | $C_{2v}$ | $C_{2v}$ |
| | $r_{U-X1(X2)}$ | 1.828 (1.9) | 1.789 (2.6) | 1.875 | 1.849 | 1.844 | 1.818 (2.0) | 1.782 (2.5) | 1.827 (1.9) |
| | $r_{U-X3}$ | 1.863 | 1.836 | 1.875 | 1.857 | 1.852 | 1.856 | 1.827 | 1.863 |
| | $\sphericalangle_{X1-U-X2}$ | 156.3 | 162.1 | 120.0 | 102.5 | 101.2 | 158.1 | 163.0 | 158.2 |
| | $\sphericalangle_{X1-U-X3}$ | 101.8 | 98.9 | 120.0 | 128.8 | 129.4 | 100.9 | 98.5 | 100.9 |
| $UO_2F$ | point group | $C_{2v}$ | $C_{2v}$ | $C_s$ | $C_s$ | $C_s$ | $C_{2v}$ | $C_{2v}$ | |
| | $r_{U-X1(X2)}$ | 1.823 | 1.795 | 1.810; 1.820 | 1.800; 1.810 | 1.796; 1.806 | 1.815 | 1.779 | |
| | $r_{U-X3}$ | 2.088 | 2.087 | 2.094 | 2.094 | 2.094 | 2.073 | 2.058 | |
| | $\sphericalangle_{X1-U-X2}$ | 169.1 | 170.1 | 170.8 | 170.3 | 170.8 | 169.6 | 171.2 | |
| | $\sphericalangle_{X1-U-X3}$ | 95.5 | 94.9 | 92.7; 96.4 | 93.0; 96.7 | 92.8; 96.3 | 95.2 | 94.4 | |
| $UOF_2$ | point group | $C_s$ | $C_1$ | $C_1$ | $C_1$ | $C_1$ | $C_s$ | $C_1$ | $C_s$ |
| | $r_{U-X1(X2)}$ | 1.840 | 1.822 | 1.837 | 1.826 | 1.823 | 1.828 | 1.817 | 1.836 |
| | $r_{U-X1(X2)}$ | 2.085 | 2.076 | 2.087 | 2.081 | 2.080 | 2.052 | 2.066 | 2.086 |
| | $r_{U-X3}$ | 2.078 | 2.071 | 2.081 | 2.074 | 2.072 | 2.050 | 2.060 | 2.082 |
| | $\sphericalangle_{X1-U-X2}$ | 160.9 | 117.3 | 114.3 | 113.7 | 114.4 | 166.4 | 117.8 | 163.1 |
| | $\sphericalangle_{X1-U-X3}$ | 105.1 | 106.9 | 104.6 | 104.3 | 104.2 | 101.9 | 107.1 | 103.8 |

  

ZORA PBE (Figure 1a). Both AE-PBE0 and AE-MP2 calculations led to a trigonal-pyramidal structure with no symmetry (Figure 1b).

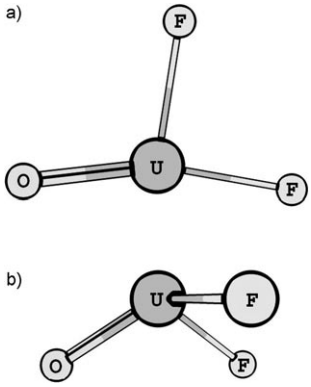


Figure 1. Structures of $UOF_2$-optimised with a) the PBE and b) the PBE0 density functionals. AE method with L1 basis set.

**$UX_5$-type (Table 3)**: The $UOF_4$ molecule is predicted to have a $C_s$ square-pyramidal geometry with the oxygen lying in the basal plane, by GGA PBE with all relativistic methods used, that is, AE, ZORA, and SC-ECP (Table 3 and Figure 2a). Hybrid functionals, as well as MP2, with both the AE and SC-ECP relativistic methods, however, give a trigonal pyramid of $C_{3v}$ symmetry (Figure 2b). No minimum corresponding to the $C_{4v}$ structure that would be similar to the one assumed by Pyykkö et al.[23] for $PuOF_4$, and to the known d elements monoxatetrafluorides $MoOF_4$ and $WOF_4$ was found. These findings are in agreement with the recent results of Kovacs and Koenigs.[31]

To our knowledge, no gas-phase experimental data on the $UOF_4$ geometry exist. Paine et al.,[69] who first obtained solid $UOF_4$, reported an X-ray structure of polymeric layers of uranium units joined by fluorine bridges with a pentagonal-bipyramidal local environment of each uranium centre. In crystals of complexes of type $UOF_4(SbF_5)_n$ which are of a similar layered type, uranium atoms also have the same configuration with oxygen and one of the fluorines in the axial positions.[70] Since these extended structures can be built by joining either square pyramidal $C_s$ or trigonal-bipyramidal $C_{3v}$ units with bridging fluorides, there is no real hint as to which computational result is correct. The potential energy surface for $UOF_4$ seems to be very shallow; the energy difference between a structures constrained to $C_{3v}$ symmetry and the fully optimised $C_s$ one at the AE-PBE/L1 level is only 0.3 kcal mol$^{-1}$. The U–F bond orders, according to the AE-DFT calculations, are slightly lower than those of $UF_6$ but still greater than unity (see Table 5).

Uranium pentafluoride is found to be a $C_{4v}$ tetragonal pyramid in all calculations. Interestingly, while AE-DFT predicted the apical U–F distance slightly shorter than the basal ones, AE-MP2 in all basis sets gives the reverse trend here. As usual, PBE gives longer uranium-to-ligand distances than PBE0. AE-MP2/L1 yields distances, which are between those of PBE and PBE0 for the same relativistic method. Increasing the basis set size for the MP2 calculations decreases all bond lengths, bringing them closer to, or, in the case of some of the U–F bonds, even shorter than those of PBE0.

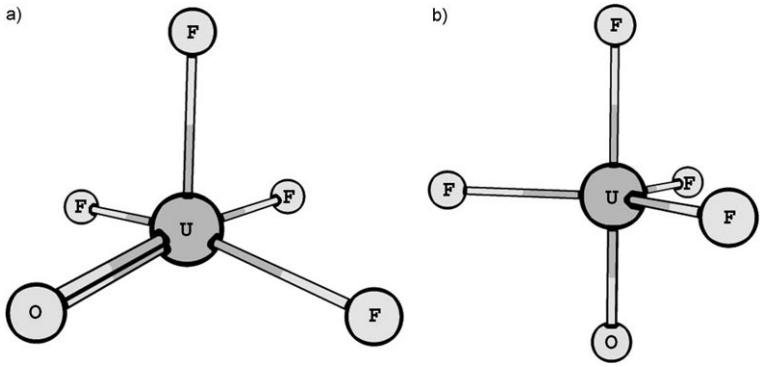


Figure 2. Structures of $UOF_4$-optimised with a) the PBE and b) the PBE0 density functionals. AE method with L1 basis set.

Table 3. Geometries of the uranium species isomorphous to $UOF_4$, calculated by different methods. Bond lengths in angstrom, angles in degrees; see Scheme 1 for numbering (geometry labels in parentheses refer to *trans* atoms); ITI% for a given bond also in parenthesis, see text for details.

| | Parameter | AE | | | | | G03, SC-RECPs | | ADF ZORA |
|---|---|---|---|---|---|---|---|---|---|
| | | PBE/L1 | PBE0/L1 | MP2/L1 | MP2/L2 | MP2/L3 | PBE/B1 | PBE0/B1 | PBE/TZP |
| $UOF_4$ | point group | $C_s$ | $C_{3v}$ | $C_{3v}$ | $C_{3v}$ | $C_{3v}$ | $C_s$ | $C_{3v}$ | $C_s$ |
| | $r_{U-X1(X2)}$ | 1.810 | 1.761 | 1.809 | 1.791 | 1.786 | 1.804 | 1.759 | 1.806 |
| | $r_{U-X2(X1)}$ | 2.014 | 1.971 | 1.993 | 1.974 | 1.968 | 2.001 | 1.961 | 2.014 |
| | | (1.9) | (3.5) | (2.9) | (3.6) | (3.8) | (2.2) | (3.6) | (2.2) |
| | $r_{U-X3(X4)}$ | 2.052 | 2.043 | 2.053 | 2.047 | 2.045 | 2.045 | 2.034 | 2.059 |
| | $r_{U-X5}$ | 2.047 | 2.043 | 2.053 | 2.047 | 2.045 | 2.039 | 2.034 | 2.052 |
| | $\sphericalangle_{X1-U-X2}$ | 170.2 | 180.0 | 180.0 | 180.0 | 180.0 | 172.0 | 180.0 | 171.3 |
| | $\sphericalangle_{X3-U-X4}$ | 166.0 | 120.2 | 120.0 | 120.0 | 120.0 | 160.6 | 120.0 | 165.3 |
| | $\sphericalangle_{X1-U-X5}$ | 99.3 | 92.3 | 91.0 | 91.1 | 91.1 | 97.7 | 92.1 | 98.1 |
| $UF_5$ | point group | $C_{4v}$ | $C_{4v}$ | $C_{4v}$ | $C_{4v}$ | $C_{4v}$ | $C_{4v}$ | $C_{4v}$ | $C_{4v}$ |
| | $r_{U-X1(X2)}$ | 2.036 | 2.017 | 2.019 | 2.010 | 2.006 | 2.027 | 2.009 | 2.039 |
| | | (−0.10) | (−0.05) | (0.14) | (0.2) | (0.3) | (−0.20) | (0.0) | (−0.25) |
| | $r_{U-X5}$ | 2.034 | 2.016 | 2.022 | 2.014 | 2.012 | 2.023 | 2.009 | 2.034 |
| | $\sphericalangle_{X1-U-X2}$ | 166.3 | 163.7 | 164.3 | 163.7 | 163.9 | 166.0 | 161.9 | 166.9 |
| | $\sphericalangle_{X1-U-X5}$ | 96.2 | 98.2 | 97.9 | 98.2 | 98.0 | 97.0 | 99.0 | 96.5 |

**$UX_4$-type (Table 4)**: $UO_2F_2$ is given by all the methods as a $C_{2v}$ see-saw molecule with the uranyl fragment slightly distorted from linearity (Figure 3a). Hybrid DFT always gives the shortest uranyl bond lengths, as well as more linear uranyls and larger F-U-F angles than other methods (Table 4). AE-DFT U−F bond orders calculated for this molecule are again slightly lower than those of $UF_6$ and $UOF_4$ (see Table 5). The decrease of the U−F bond order agrees with the increase of the U−F bond ionicity with substituting neighbouring fluorine atoms to oxygens as noted by Kovacs et al.[30]

Uranium tetrafluoride is slightly distorted from a regular tetrahedral configuration as previously reported.[18,30] Different methods give slightly different distortions. AE methods yield a scissor-like distortion with all U−F distances being equivalent; SC-ECP DFT methods give $C_{2v}$ structures; ADF ZORA even a $C_{3v}$ structure. We note that the ADF ZORA calculations had a rather moderate quality of integration and optimisation criteria. Differences in energies between distorted and regular tetrahedral geometries are, however, expected to be small in each case.[18]

Table 4. Geometries of the uranium species isomorphous to $UO_2F_2$, calculated by different methods. Bond lengths in angstrom, angles in degrees; see Scheme 1 for numbering (geometry labels in parentheses refer to *trans* atoms); ITI % for a given bond also in parenthesis, see text for details.

| | Parameter | AE | | | | | G03, SC-RECPs | | ADF ZORA |
|---|---|---|---|---|---|---|---|---|---|
| | | PBE/L1 | PBE0/L1 | MP2/L1 | MP2/L2 | MP2/L3 | PBE/B1 | PBE0/B1 | PBE/TZP |
| $UO_2F_2$ | point group | $C_{2v}$ | $C_{2v}$ | $C_{2v}$ | $C_{2v}$ | $C_{2v}$ | $C_{2v}$ | $C_{2v}$ | $C_{2v}$ |
| | $r_{U-X1(X2)}$ | 1.800 | 1.760 | 1.801 | 1.785 | 1.780 | 1.793 | 1.756 | 1.797 |
| | $r_{U-X3(X4)}$ | 2.068 | 2.058 | 2.071 | 2.064 | 2.063 | 2.056 | 2.047 | 2.079 |
| | $\measuredangle_{X1-U-X2}$ | 168.2 | 170.7 | 169.5 | 169.6 | 170.2 | 169.1 | 171.0 | 168.3 |
| | $\measuredangle_{X3-U-X4}$ | 111.2 | 115.0 | 111.0 | 110.9 | 111.5 | 112.7 | 115.5 | 111.8 |
| | $\measuredangle_{X1-U-X5}$ | 93.3 | 92.5 | 93.0 | 93.0 | 92.7 | 93.0 | 92.4 | 93.3 |
| $UOF_3$ | point group | $C_s$ | $C_s$ | $C_s$ | $C_s$ | $C_s$ | $C_s$ | $C_s$ | $C_s$ |
| | $r_{U-X1(X2)}$ | 1.819 | 1.787 | 1.801 | 1.788 | 1.784 | 1.814 | 1.784 | 1.827 |
| | $r_{U-X2(X1)}$ | 2.046 | 2.028 | 2.030 | 2.016 | 2.010 | 2.034 | 2.018 | 2.054 |
| | | (0.3) | (0.7) | (1.1) | (1.5) | (1.7) | (0.5) | (0.7) | (0.3) |
| | $r_{U-X3(X4)}$ | 2.053 | 2.042 | 2.053 | 2.046 | 2.044 | 2.044 | 2.032 | 2.060 |
| | $\measuredangle_{X1-U-X2}$ | 163.6 | 162.6 | 165.5 | 165.9 | 166.7 | 164.1 | 162.5 | 163.1 |
| | $\measuredangle_{X3-U-X4}$ | 103.2 | 104.8 | 104.3 | 104.1 | 104.2 | 102.4 | 105.2 | 103.8 |
| | $\measuredangle_{X1-U-X3}$ | 98.3 | 98.9 | 97.6 | 97.4 | 97.2 | 99.3 | 98.7 | 98.5 |
| $UF_4$ | point group | $C_1$ | $C_1$ | $C_1$ | $C_1$ | $C_1$ | $C_{2v}$ | $C_{2v}$ | $C_{3v}$ |
| | $r_{U-X1(X2)}$ | 2.062 | 2.051 | 2.061 | 2.054 | 2.052 | 2.049 | 2.039 | 2.075 |
| | $r_{U-X2(X1)}$ | 2.062 | 2.051 | 2.061 | 2.054 | 2.052 | 2.049 | 2.039 | 2.049 |
| | $r_{U-X3(X4)}$ | 2.062 | 2.051 | 2.061 | 2.054 | 2.052 | 2.056 | 2.045 | 2.075 |
| | $\measuredangle_{X1-U-X2}$ | 106.0 | 106.2 | 106.1 | 106.5 | 106.0 | 105.8 | 105.8 | 105.5 |
| | $\measuredangle_{X3-U-X4}$ | 106.0 | 106.2 | 106.1 | 106.0 | 105.9 | 104.9 | 104.7 | 113.1 |
| | $\measuredangle_{X1-U-X5}$ | 116.6 | 116.3 | 116.6 | 116.6 | 116.7 | 111.6 | 111.6 | 113.2 |

Similarly to it, $UOF_3$ has an almost linear O=U-F fragment and two "see-saw" fluorines in an orthogonal plane to it, with an overall $C_s$ symmetry, for all the methods (Figure 3b).

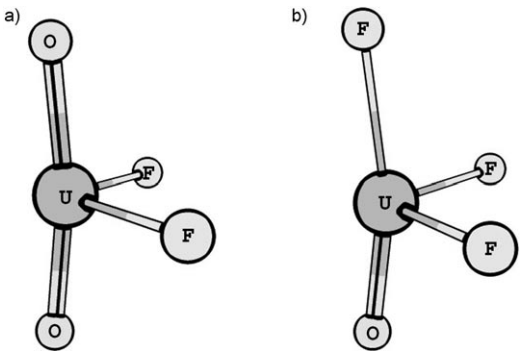


Figure 3. Structures of a) $UO_2F_2$ and b) $UOF_3$ optimised with the PBE density functional. AE method with L1 basis set.

### ITI, covalency and stereochemistry of uranium oxofluorides

Bond orders[63] and atomic Hirshfeld charges[64] are provided in Table 5 for all the uranium compounds studied. In comparing the different DFT methods, a general trend becomes apparent: The hybrid PBE0 method gives consistently higher charges on atoms and lower population bond orders between them than the pure GGA PBE. We note that, at the same time, the PBE0 bond lengths are always lower than those of PBE (Tables 1–4). Thus, geometry (and therefore overlap integrals) differences cannot be the reason for the differences in bond orders. Instead, the overall picture of bond orders together with the charges means that hybrid DFT predicts structures to be more "ionic" and less "covalent" than does a pure GGA. Nonetheless, bond orders for U−F bonds are always higher than unity even for the all-electron hybrid DFT method. This suggests a significant back-donation from the lone pairs at the fluorine atoms to the metal atom. U=O bonds always have bond orders between two and three independent of how many there are in a given molecule (one, two or three).

Despite these differences in the ionicity of the bonds, the qualitative trends given by PBE0 and PBE are the same. For example, the transition from $U^{VI}$ to $U^{IV}$ in similar rows of compounds—such as $UF_6 > UF_5 > UF_4$ and $UOF_4 > UOF_3 > UOF_2$, and $UO_2F_2 > UO_2F$—decreases the U−F bond orders. The U−F bond orders also decrease in rows of a given oxidation state of the metal but with increasing content of oxygen, that is, $UF_6 > UOF_4 > UO_2F_2$; and $UF_5 > UOF_3 > UO_2F$. The latter trend can be explained as a competition for bonding between oxygen and fluorine lone pairs: the more oxygen pairs are bound to the uranium, the less it does require back-donation from fluorines, and the more ionic the remaining U−F bonds become. The Hirshfeld

  

Table 5. Population bond orders (b/o) and Hirshfeld charges ($q$) for uranium oxofluorides as calculated by selected AE-DFT methods. In parenthesis are ligands *trans* to a given atom/bond.

| | | PBE/L1 | PBE0/L1 | | | PBE/L1 | PBE0/L1 |
|---|---|---|---|---|---|---|---|
| $UF_6$ | $b/o_{(U-F)}$ | 1.28 | 1.19 | $UF_4$ | $b/o_{(U-F)}$ | 1.21 | 1.09 |
| | $q_U$ | 0.859 | 1.050 | | $q_U$ | 0.920 | 1.082 |
| | $q_F$ | −0.143 | −0.175 | | $q_F$ | −0.230 | −0.271 |
| $UO_3$ | $b/o_{(U=O)}$ | 2.44(O); 2.48 | 2.35(O); 2.39 | $UF_5$ | $b/o_{(U-F)}$ | 1.27(F); 1.24 | 1.16(F); 1.13 |
| | $q_U$ | 0.989 | 1.085 | | $q_U$ | 0.907 | 1.091 |
| | $q_O$ | −0.327(O); −0.335 | −0.352(O); −0.381 | | $q_F$ | −0.180(F); −0.187 | −0.216(F); −0.225 |
| $UOF_4$ | $b/o_{(U=O)}$ | 2.45 | 2.39 | $UOF_3$ | $b/o_{(U=O)}$ | 2.47 | 2.39 |
| | $b/o_{(U-F)}$ | 1.26(O,F); 1.23 | 1.19(O); 1.14 | | $b/o_{(U-F)}$ | 1.23; 1.24(O) | 1.11; 1.14(O) |
| | $q_U$ | 0.933 | 1.115 | | $q_U$ | 0.936 | 1.086 |
| | $q_O$ | −0.238 | −0.242 | | $q_O$ | −0.310 | −0.338 |
| | $q_F$ | −0.179(F); −0.151(O); −0.119; | −0.161(O); −0.237 | | $q_F$ | −0.212(F); −0.201(O) | −0.256(F); −0.236(O) |
| $UO_2F_2$ | $b/o_{(U=O)}$ | 2.41 | 2.34 | $UO_2F$ | $b/o_{(U=O)}$ | 2.41 | 2.33 |
| | $b/o_{(U-F)}$ | 1.24 | 1.11 | | $b/o_{(U-F)}$ | 1.20 | 1.07 |
| | $q_U$ | 0.983 | 1.121 | | $q_U$ | 0.940 | 1.057 |
| | $q_O$ | −0.282 | −0.299 | | $q_O$ | −0.345 | −0.378 |
| | $q_F$ | −0.210 | −0.261 | | $q_F$ | −0.250 | −0.301 |
| $UO_2$ | $b/o_{(U=O)}$ | 2.43 | 2.36 | $UOF_2$ | $b/o_{(U=O)}$ | 2.46 | 2.36 |
| | $q_U$ | 0.684 | 0.728 | | $b/o_{(U-F)}$ | 1.22; 1.23(O) | 1.08 |
| | $q_O$ | −0.342 | −0.364 | | $q_U$ | 0.835 | 1.005 |
| | | | | | $q_O$ | −0.360 | −0.421 |
| | | | | | $q_F$ | −0.240; −0.235(O) | −0.291; −0.293 |

charges also confirm this trend. The former trend reflects the obvious increase in the ionic character of the bonds with the decrease of the oxidation state of the central atom and therefore its ability to polarize ligand anions.

Let us consider the geometries of the complexes in more detail. The inverse *trans*-influence (ITI), that is, an effect inverse to the *trans*-influence known in the chemistry of d elements, is an effect of shortening/stabilisation of the uranium-to-ligand bond *trans* to (usually) an oxygen ligand. A simple explanation of ITI was given by Denning:[71] The basis of this explanation is treating "the effect of the ligand, viewed as an anion, as a simple electrostatic perturbation acting on core electrons." At this point, a distinction is made between atoms having the same and opposite parity between highest filled core orbitals and the lowest empty valence orbitals, respectively. The latter case leads to dominantly dipolar interactions and accumulation of negative charge in the *trans* position. Most of the d elements fall in this category. In the former case that applies to the f elements, the dominant interaction "is likely to be *quadrupolar* [polarisation], with an accumulation of electronic charge in the *cis* position." This stabilizes the *trans* position and leads to the ITI. (Quotes from Denning[71]).

O'Grady and Kaltsoyannis[72] studied ITI using GGA DFT methods applied to octahedral actinide complexes $AnOX_5^{n-}$, and Kovacs and Konings discussed it in their work on $UOX_4$ complexes.[31] As a quantitative measure of ITI, the relative length of *trans* to *cis* ligand in $AnOX_5^{n-}$ (in percent) was proposed by Kaltsoyannis, while the latter authors[31] chose relative shortening $(100\,\% - R_{(U-X)}^{trans}/R_{(U-X)}^{cis} \times 100\,\%)$ as a more illustrative indicator of ITI: that is, the larger it is, the stronger the effect. We note here that, in going from octahedral $AnOX_5^{n-}$ complexes to less symmetric ones such as those studied in our work, the ITI value will include some other components, since different ligand positions in a complex might have been influenced, in addition to ITI, by steric interactions or charge–charge repulsion with neighbouring ligands.

Nonetheless, we calculated the ITI for some of our compounds using the formula of Kovacs and Konings.[31] (The values are provided in Tables 2–4 in parentheses next to the bonds under consideration.) We note that, according to all our methods, there is a pronounced ITI in our compounds in which there is a fluorine *trans* to a U=O group especially for $UOF_4$ and $UOF_3$. The see-saw geometry of the former is likely a direct result of the ITI stabilisation. Both the hybrid PBE0 functional and the MP2 method show higher ITI values than the GGA PBE for all the relativistic methods; increasing the basis set with MP2 not only makes all bonds shorter, as it was noted above, but also increases the ITI.

One can also consider ITI in the T-shaped $UO_3$ molecule, comparing the bond lengths of the "uranyl" oxygens with the "oxide" oxygen. The ITI is high in this case, according to PBE and PBE0. The ITI of the fluorine ligand can be traced for the $UF_5$ example, comparing basal U–F lengths (which have roughly a *trans* ligand, another F) with the apical one. The effect of fluorine is much weaker than for the oxygen ligands, according to the MP2 method which yielded small ITI increasing with basis set size. For the DFT methods it is even predicted to be negative (i.e., being normal *trans*-influence).

One can note that the more ionic/less covalent charge distribution given by hybrid DFT corresponds to more highly pronounced inverse *trans*-influence in the geometries of the complexes. (The effect is probably similar for MP2: We don't have charges from a perturbed wavefunction implemented yet in the Priroda AE code, but HF is known to give even more "ionic" results than its 25 % hybrids, and 2nd order corrections are unlikely to change this.) The higher the charges given by a method, the stronger the ITI affects the geometries, which is in accordance with Den-

  

ning's picture of the ITI as discussed above.[71] At the same time we note that the ITI effect is strong for $U^{VI}$ compounds but gets less pronounced for lower valent complexes (comparing for example, $UOF_4$ and $UOF_3$).

### Vibrational constants of the molecules

Frequencies of uranyl groups and U=O bonds are very characteristic. They change systematically with the change in neighbouring groups and are available from several experimental sources. For the sake of brevity, we will consider only those frequencies for the molecules we study. Calculated and experimental frequencies, where available, are provided in Table 6.

Table 6. Calculated and experimental U=O vibrational wavenumbers of the uranium oxides and oxofluorides (in $cm^{-1}$).

| Molecule/ vibration | AE | | | | G03, SC-RECPs | | | ADF ZORA | Expt. |
|---|---|---|---|---|---|---|---|---|---|
| | PBE/ L1 | PBE0/ L1 | MP2/ L1 | MP2/ L2 | PBE/ B1 | PBE0/ B1 | PBE0/ B2 | PBE/TZP | |
| $UOF_4$, $\nu_{U=O}$ | 855.1 | 947.1 | 863.9 | 874.5 | 869.6 | 963.4 | 972.2 | 865.0 | 834.7 |
| $UOF_3$, $\nu_{U=O}$ | 845.5 | 909.7 | 898.7 | 900.5 | 852.1 | 918.6 | 930.3 | 849.4 | |
| $UOF_2$, $\nu_{U=O}$ | 831.1 | 882.8 | 856.9 | 867.0 | 838.1 | 889.0 | 894.9 | 816.2 | |
| $UO_2F_2$, $\nu_{O=U=O}^{sym}$ | 845.1 | 925.6 | 831.9 | 847.6 | 858.9 | 940.1 | 949.0 | 850.2 | |
| $UO_2F_2$, $\nu_{O=U=O}^{asym}$ | 913.6 | 992.4 | 925.9 | 943.9 | 934.9 | 1015.4 | 1018.7 | 923.5 | 940.5 |
| $UO_2F$, $\nu_{O=U=O}^{sym}$ | 820.3 | 881.6 | 814.9 | 820.4 | 831.3 | 902.8 | 900.0 | | |
| $UO_2F$, $\nu_{O=U=O}^{asym}$ | 878.7 | 927.2 | 895.2 | 905.3 | 896.7 | 938.4 | 920.4 | | 871.7 |
| $UO_3$, $\nu_{O=U=O}^{sym}$ | 848.6 | 919.3 | 762.8 | 779.3 | 869.6 | 930.1 | 935.1 | 849.0 | 852.6 |
| $UO_3$, $\nu_{O=U=O}^{asym}$ | 849.3 | 921.1 | 780.6 | 785.6 | 852.1 | 947.8 | 944.1 | 850.4 | 843.5 |
| $UO_3$, $\nu_{U=O}$ | 764.8 | 815.7 | 780.8 | 815.1 | 768.0 | 826.8 | 824.3 | 758.3 | 745.6 |
| $UO_2$, $\nu_{O=U=O}^{sym}$ | 815.1 | 903.6 | 803.3 | 808.7 | | 923.0 | 921.0 | | |
| $UO_2$, $\nu_{O=U=O}^{asym}$ | 899.2 | 959.3 | 918.9 | 927.5 | | 987.7 | 980.2 | | 914.8 |
| mean error[a] | 0.8 | 68.4 | −10.8 | 4.0 | 17.1 | 86.6 | 84.5 | 5.9 | |
| M.A.E.[a] | 14.1 | 68.4 | 37.0 | 41.5 | 18.9 | 86.6 | 84.5 | 14.1 | |

[a] Taking only those frequencies into account where experimental data exists; M.A.E. = mean absolute error.

First, we note that for U=O frequencies, PBE in combination with all the relativistic methods give close values. The maximal difference, which is between the AE-PBE/L1 and SC-ECP PBE/B1 results, is 21.3 $cm^{-1}$. For the PBE0 functional, differences between AE and SC-ECP methods for the same basis sets are slightly bigger. SC-ECP DFT systematically gives larger values than the AE and ZORA methods. This is probably a basis set effect; the PBE0/B2 frequencies are in most cases slightly higher that PBE0/B1 ones. Frequencies given by MP2/L2 basis are always 5–10 $cm^{-1}$ higher than those of MP2/L1.

Second, hybrid DFT systematically gives higher values than GGA. Differences range from 50 to 90 $cm^{-1}$, and extending the basis set, for SC-ECP PBE0, does not amend it. MP2 does not overestimate frequencies as much as PBE0, and the differences between MP2 and PBE values are not as big (except for the case of $UO_3$ in which the molecular symmetry is different for these methods).

Third, agreement with experiment is better for the GGA than for the hybrid DFT. The latter overestimates the vibrational frequencies systematically. This is clearly evident from the mean unsigned and absolute errors.

It is interesting to look at trends in uranyl frequencies with stepwise fluorine removal from $UOF_4$ and $UO_2F_2$. These trends could be of some practical importance because it is sometimes hard to distinguish experimentally between, for example, $UOF_4$ and $UOF_2$. One can see that in the row $UOF_4$, $UOF_3$, $UOF_2$ there is a decrease in U=O frequency according to all DFT methods used. AE-MP2, however, predicts a different order with the $UOF_4$ wavenumber being the lowest. In the row $UO_2F_2$, $UO_2F$, $UO_2$ the trend is slightly different: the asymmetric O=U=O stretch frequency decreases for $UO_2F$ but becomes higher again for $UO_2$. This qualitatively reproduces the available experimental trend (Table 6).

### Energetics

Standard enthalpies of the reactions (1) to (15), calculated by different relativistic methods as well as derived from experimental values, are collected in Table 7.

**Homolytic dissociation reactions**: First, we will consider the dissociation processes reactions (4) to (12). One can see that the GGA PBE functional gives close values for both the U−F and U=O bond dissociation energies (BDE) with all three different relativistic methods used: AE scalar four component, SC-ECP and ZORA. Results given by hybrid DFT functional are also close for the two relativistic methods available, AE and SC-ECP. The SC-ECP results show some basis set dependence with the larger B2 basis set giving somewhat lower bond dissociation energies (BDEs), Table 7. We did not extend our calculations to basis sets larger than B2 due to high computational demands of the SC-ECP implementation in the code we used and basis linear dependence problems arising. The hybrid functional PBE0 predicts lower dissociation energies than PBE for both the AE four-component and SC-ECP relativistic methods.

Comparing the PBE and PBE0 results against the "experimental" data, one can see that the best agreement is given by the hybrid PBE0 density functional. For the U−F bond dissociation in $UF_6$ and $UF_5$ [i.e., reactions (4) and (5)] the good agreement of hybrid DFT (used with both small-core ECPs and third-order Douglas–Kroll–Hess relativistic methods) with the experiment was reported already by Batista et al.[18] Here, we report that the enthalpy of dissociation of the U=O bonds in $UOF_4$ and $UO_3$ [reactions (8) and (12)], as well as the dissociation of fluorine atoms next to uranyl

  

Table 7. Calculated and experimental reaction enthalpies at 298.15 K (in kcal mol$^{-1}$).

| Reaction number | AE | | | G03, SC-RECPs | | | | ADF ZORA | Expt. |
|---|---|---|---|---|---|---|---|---|---|
| | PBE/L1 | PBE0/L1 | MP2/L1 | PBE/B1 | PBE/B2 | PBE0/B1 | PBE0/B2 | PBE/TZP | |
| 1 | −44.7 | −70.1 | −67.0 | −43.1 | −47.5 | −68.1 | −72.5 | −47.2 | −74.6 |
| 2 | 5.9 | 5.0 | −5.5 | 6 | 5.4 | 4.3 | 4.0 | 5.3 | 7.2 |
| 3 | −25.3 | −37.5 | −30.8 | −24.6 | −26.4 | −36.2 | −38.3 | −26.2 | −40.9 |
| 4 | 100.5 | 73.6 | 84.0 | 107.07 | 100.8 | 80.65 | 76.3 | 101.5 | 71.0 |
| 5 | 120.8 | 97.8 | 97.8 | 127.38 | 120.9 | 105.14 | 99.8 | 126.6 | 98.0 |
| 6 | 111.2 | 89.9 | 106.0 | 118.4 | 112.6 | 97.5 | 93.4 | 112.8 | |
| 7 | 248.5 | 211.6 | 234.6 | 261.4 | 251.1 | 225.6 | 217.3 | 252.5 | |
| 8 | 132.6 | 95.3 | 120.9 | 134.9 | 131.8 | 97.8 | 97.4 | 137.7 | 91.3 |
| 9 | 126.2 | 110.4 | 125.1 | 132.8 | 127.3 | 117.1 | 114.4 | | |
| 10 | 266.2 | 241.9 | 249.9 | | | 254.6 | 248.6 | | 248.6 |
| 11 | 165.7 | 140.5 | 168.2 | 167.9 | 166.6 | 153.3 | 142.5 | 167.5 | |
| 12 | 158.0 | 133.3 | 152.7 | | | 134.8 | 135.6 | | 138.0 |
| 13 | 43.2 | 33.2 | 11.8 | 59.6 | 53.9 | 49.1 | 45.7 | 38.3 | 25.9 |
| 14 | 80.5 | 61.5 | 29.1 | 113.2 | 75.4 | 93.8 | 60.0 | 71.4 | 44.6 |
| 15 | 143.1 | 127.3 | 77.2 | 191.3 | 136.9 | 174.7 | 126.2 | 130.6 | 104.1 |
| mean error[a] | 24.3 | 4.4 | 0.6 | 38.4 | 25.0 | 16.1 | 6.3 | 23.5 | |
| M.A.E.[a] | 24.6 | 6.9 | 13.2 | 38.6 | 25.4 | 17.2 | 7.3 | 23.9 | |

[a] Taking only those reactions into account where experimental data exists; M.A.E. = mean absolute error.

in $UO_2F_2$ [reaction (10)], are reproduced by the PBE0 functional equally well. The pure GGA PBE functional strongly overestimated BDEs for both types of bonds. We note (Table 7) that discrepancies between PBE-calculated and experimental enthalpies (and, where the latter being unavailable, the enthalpies given by the PBE0 functional as the most reliable) are sometimes different for different molecules. BDEs for reactions of oxygen dissociation from $UOF_4$ [reaction (8)], as well as both first and second fluorine dissociations from $UOF_4$ and $UF_6$, are overestimated much stronger than for the corresponding processes of $UO_2F_2$. It seems that GGA DFT overestimates the stability of compounds with a higher content of fluorine.

To test the possible influence of the selection of the GGA density functional on the thermochemistry of the systems studied, we have recalculated our complexes with the MPBE, BPBE, BLYP and OLYP exchange-correlation functionals (see Computational Methods above) using the AE scalar relativistic method and the L1 basis set. Molecular geometries given by all these functionals were found similar to the ones obtained by PBE. For the "troublesome" cases of $UOF_4$, $UOF_2$, and $UO_3$, these GGA functionals give the same configurations of the complexes as PBE. Calculated enthalpies of the reactions (1)–(15) are provided in the Table 8. For the L1 basis set, the MPBE functional gives values very close to PBE (differences are less than 4 kcal mol$^{-1}$). The BPBE and BLYP functionals give somewhat lower values (up to 10 kcal mol$^{-1}$) for the dissociation energies. The largest changes in dissociation energies, compared with PBE, are given by OLYP functional, which gives the lowest BDEs for U−F and U=O bonds amongst the tested functionals. However, even the OLYP results are still away from the experimental BDE values. Thus, none of the tested GGA functionals performed nearly as good as the hybrid PBE0 functional. In order to test the convergence of energies with respect to the basis set, we repeated the AE calculations with the PBE and OLYP functionals using the L2 quality basis set (see Table 8). For both functionals, energies of the reactions (4)–(12) calculated with L2 basis set are only slightly different (higher) than those of L1 basis. Since the differences are really small, we can conclude that GGA results are quite converged with respect to the basis set size.

The AE-MP2/L1 calculations (Table 7) give reaction energies between the ones obtained by the PBE and PBE0 methods for most of these reactions. We note that differences between this method and the DFT ones are not uniform. For the reactions (4) and (5) and (10) which correspond to U−F dissociation they are closer to the PBE0 results, while in other cases, they are closer to the PBE ones.

Table 8. Reaction enthalpies calculated by different GGA functionals and basis sets, and experimental reaction enthalpies at 298.15 K (in kcal mol$^{-1}$).

| Reaction number | AE, L1 | | | | | AE, L2 | | Expt. |
|---|---|---|---|---|---|---|---|---|
| | PBE | MPBE | BPBE | BLYP | OLYP | PBE | OLYP | |
| 1 | −44.7 | −44.8 | −45.1 | −42.7 | −47.4 | −47.0 | −49.7 | −74.6 |
| 2 | 5.9 | 5.7 | 5.6 | 4.7 | 5.4 | 5.3 | 4.8 | 7.2 |
| 3 | −25.3 | −25.2 | −25.4 | −23.7 | −26.4 | −26.2 | −27.2 | −40.9 |
| 4 | 100.5 | 98.2 | 94.5 | 96.4 | 89.4 | 100.8 | 90.6 | 71.0 |
| 5 | 120.8 | 118.5 | 114.8 | 116.8 | 109.2 | 120.8 | 110.3 | 98.0 |
| 6 | 111.2 | 109.1 | 105.5 | 107.8 | 101.0 | 112.2 | 102.8 | |
| 7 | 248.5 | 244.4 | 237.5 | 241.6 | 228.8 | 251.1 | 233.0 | |
| 8 | 132.6 | 129.5 | 125.3 | 124.2 | 117.4 | 132.6 | 119.1 | 91.3 |
| 9 | 126.2 | 124.1 | 120.6 | 122.6 | 116.7 | 127.7 | 118.9 | |
| 10 | 266.2 | 262.5 | 256.1 | 259.0 | 250.9 | 269.9 | 255.8 | 248.6 |
| 11 | 165.7 | 162.9 | 159.2 | 157.3 | 153.1 | 167.4 | 156.0 | |
| 12 | 158.0 | 155.8 | 152.5 | 151.0 | 148.7 | 160.0 | 151.5 | 138.0 |
| 13 | 43.2 | 42.2 | 38.7 | 44.1 | 33.9 | 40.0 | 30.3 | 25.9 |
| 14 | 80.5 | 78.6 | 71.8 | 83.5 | 62.4 | 74.7 | 55.9 | 44.6 |
| 15 | 143.1 | 140.3 | 130.2 | 146.6 | 117.4 | 135.6 | 108.7 | 104.1 |
| mean error[a] | 24.3 | 22.6 | 18.7 | 22.4 | 13.4 | 23.0 | 12.4 | 24.3 |
| M.A.E.[a] | 24.6 | 22.8 | 19.0 | 22.9 | 13.8 | 23.4 | 12.9 | 24.6 |

[a] See footnote [a] to Table 7.

Table 9. Reaction enthalpies calculated by all-electron scalar relativistic MP2 with basis sets L1–L3 and complete basis set (CBS) approximation, CCSD(T) and experimental reaction enthalpies at 298.15 K (in kcal $mol^{-1}$).

| Reaction number | AE-MP2 | | | | AE-CCSD(T)/L1//MP2/L3 | AE-CCSD(T) corrected[a] | Expt. |
|---|---|---|---|---|---|---|---|
| | L1 | L2 | L3 | CBS | | | |
| 1 | −67.0 | −73.5 | −75.0 | −77.4 | −91.2 | −101.7 | −74.6 |
| 2 | −5.5 | −5.9 | −5.9 | −6.2 | −0.5 | −1.1 | 7.2 |
| 3 | −30.8 | −33.8 | −34.5 | −35.6 | −45.4 | −50.3 | −40.9 |
| 4 | 84.0 | 87.7 | 88.9 | 88.6 | 69.1 | 73.8 | 71.0 |
| 5 | 97.8 | 103.2 | 104.4 | 104.4 | 92.2 | 98.9 | 98.0 |
| 6 | 106.0 | 111.0 | 112.1 | 112.3 | 90.8 | 97.0 | |
| 7 | 234.6 | 245.4 | 248.0 | 248.9 | 210.5 | 224.8 | |
| 8 | 120.9 | 125.3 | 126.9 | 127.4 | 95.5 | 102.0 | 91.3 |
| 9 | 125.1 | 130.0 | 131.2 | 132.6 | 115.1 | 122.6 | |
| 10 | 249.9 | 264.8 | 269.9 | 273.4 | 237.8 | 261.3 | 248.6 |
| 11 | 168.2 | 173.8 | 175.7 | 177.0 | 144.2 | 153.0 | |
| 12 | 152.7 | 159.5 | 163.1 | 165.9 | 126.2 | 139.2 | 138.0 |
| 13 | 11.8 | 11.9 | 11.8 | 10.4 | 20.8 | 19.6 | 25.9 |
| 14 | 29.1 | 29.7 | 29.6 | 27.0 | 42.0 | 40.3 | 44.6 |
| 15 | 77.2 | 81.3 | 81.9 | 79.2 | 108.6 | 111.3 | 104.1 |
| mean error[b] | 0.6 | 3.4 | 4.4 | 4.0 | −5.3 | −1.8 | |
| M.A.E.[b] | 13.2 | 15.1 | 16.1 | 17.5 | 6.9 | 8.3 | |

[a] Estimated correction for basis set effects added, see the text. [b] See footnote [a] to Table 7.

MP2 energies with the bigger basis sets L2 and L3, as well as extrapolated complete basis set (CBS) values, are summarised in Table 9. Not surprisingly, differences between BDEs calculated with L1 and L2 bases are significantly higher for MP2 than for PBE (see Table 8 and discussion above); results in the large L3 basis look more converged and don't differ much from the CBS-approximated values. Increasing the basis leads to increasing bond dissociation energies. Thus the final L3 and CBS values of the BDE get shifted towards the PBE results compared with the MP2/L1 numbers from Table 7. (In the case of the U−F dissociations from $UOF_4$ and $UO_2F_2$, the MP2/CBS BDE values actually become even higher than those of PBE.) Still, even for MP2/CBS we note that the errors (compared with the experimental results) in U−F and U=O bond energies are different—with the former [reactions (4), (5), (10)] being less overestimated than the latter [reactions (8) and (12)]. This is in contrast with the overall picture for hybrid DFT methods (and somewhat opposite to the GGA results which tended to overbind highly-fluorinated uranium complexes stronger). Comparing the MP2/L3 and MP2/CBS results with the PBE0 ones as most reliable, we also find that MP2 relatively overestimates both the first and second BDEs for U−F bonds in oxygen-containing molecules $UOF_4$ and $UO_2F_2$ much stronger compared with the corresponding BDEs in $UF_6$.

After considering the absolute values of the dissociation energies, it is interesting to see whether our methods reproduce qualitative trends along some rows of our uranium oxofluorides. First, all the methods predicted that dissociation of the second fluorine from a complex requires more energy than for the first one. This is in agreement with the known experimental trend for $UF_n$.[8] The calculations show that removal of an oxygen atom takes more energy than of a fluorine, but less than for two fluorines. In the cases of $UOF_4$ and $UO_3$ there are corresponding experimental data available, which confirm this observation. In the row $UF_6 < UOF_4 < UO_2F_2$, the BDE for both first and second fluorine increases according to both DFT methods, as well as for the AE-MP2 method. Although we don't have the experimental data for $UOF_4$, experimental data points available for $UO_2F_2$ and $UF_6$ [Table 5, reactions (4), (5), (10)] confirm the trend. As was mentioned above, increasing the number of oxygen atoms in this row makes the neighboring U−F bonds more ionic and stronger.

In the row $UOF_4$, $UO_2F_2$, $UO_3$, the dissociation of an oxygen atom is the easiest for the first one; but the hardest for the dioxodifluoro complex. This is an obvious result of the stability of the uranyl moiety. The dissociation energy of the odd oxygen of the uranium trioxide is closer to the one of $UO_2F_2$ than to the oxygen of $UOF_4$. This can be understood considering the partial triple-bond character of all of U=O bonds in the $UO_3$ molecule, as well as the inverse *trans*-influence which destabilizes the odd oxygen ligand because it is *cis* to the two uranyl ones (see above).

**Conproportionations and hydrolysis reactions**

For the dissociation processes considered above one or more of the reagents and products have unpaired electrons. Treating open-shell systems with the unrestricted HF approach is known to create some error due to spin contamination, especially for the MP2 method. Moreover, in cases where these unpaired electrons are f electrons of uranium, spin-orbit and multiplet effects most certainly will have some influence on the calculated reaction enthalpies.

It is possible, however, to consider oxide and fluoride conproportionation processes such as (1)–(3), as well as hydrolysis reactions (13)–(15). These reactions involve only closed-shell compounds of uranium(VI) for which spin-orbit effects are known to be negligible. At the same time, the energies of these processes do reflect the relative strengths of the U−F and U=O bonds. These BDEs were discussed in the previous paragraphs of this work. By comparison of the trends in the relative U=O and U−F bond strengths, it is possible to evaluate whether or not our calculated BDEs are artifacts of the scalar relativistic or unrestricted HF approaches.

Calculated enthalpies for the reactions (1)–(3) and (13)–(15) are provided in Tables 7–9. First, we consider the con-

  

proportionation reactions (1)–(3). The energies of those reactions can be roughly understood in terms of changes of the U−F and U=O bond energies with the environment of the central atom: According to the BDE calculations above, U−F bonds get stronger with an increase of the oxygen content in the molecule. U=O bonds in the difluorodioxo–uranium are the strongest. Because of that, formation of the $UO_2F_2$ product from the more highly fluorinated complexes [reactions (1) and (3)] must be a thermodynamically favorable act. The reaction (2) should be endothermic, for the U=O bond in $UOF_4$ is weaker than in $UO_2F_2$, and the U−F bonds in $UO_2F_2$ are stronger than in both $UOF_4$ and $UF_6$.

Results from Table 7 show that, just as for the dissociation reactions, different relativistic methods yield similar results for a given DFT functional. The hybrid functional PBE0 again gives the best agreement with the experimental values for all three conproportionation reactions. While the enthalpy of reaction (2) agrees with the experimental data for the pure GGA PBE functional, its results for reactions (1) and (3) underestimate the exothermicity. This could be explained as a result of the stronger overbinding tendency, noted above for BDEs, of the GGA functional for fluorine-rich complexes, which are on the left hand side of reaction (1) and (3). All GGA functionals with the AE relativistic method (Table 8) give very similar results.

For the reactions (1) and (3), the AE-MP2 method gives values close to the experiment. However, reaction (2) is incorrectly predicted as exothermic. This is a result of the overestimation of the U−F bond energies in $UOF_4$ and $UO_2F_2$ compared with the ones in $UF_6$ by this method. This was noted above for the corresponding BDEs.

The overall picture of how the enthalpies of reactions (1)–(3) depend on the correlation method used is very interesting: It means that these reactions are very non-isodesmic, even though they might appear isodesmic at the first sight, and therefore require a proper correlation method to be used.

Second, let's consider the hydrolysis reactions (13)–(15). The gas-phase hydrolysis of uranium hexafluoride was correctly predicted to be endothermic by all methods used herein. In general, DFT methods have more endothermic energies for these reactions (Tables 7 and 8), while MP2 (Table 9) underestimates the endothermicity compared with the "experimental" data. This follows the trend in dissociation energies predicted by these methods: MP2 tends to overestimate BDEs for U=O bonds as well as U−F bonds in oxygen-containing complexes much more than U−F bonds in $UF_6$ and $UF_5$. Because the $UF_6$ hydrolysis reactions have each two U−F bonds substituted by one U=O bond, the error of the MP2 method is thus not completely cancelled out. We note that for hydrolysis reactions MP2 results do not change as significantly with basis set increase as for the other reactions studied here.

The AE scalar relativistic PBE0/L1 method gives slightly better results than AE-PBE, probably due to smaller errors for the former for both U=O and U−F bond energies. However, reactions (13)–(15) are still predicted to be too exothermic compared with the experiment. We note that AE calculation with the OLYP functional, especially in the L2 basis, provided the best agreement with the experiment (Table 8). This might be due to fortuitous error cancellation in the U−F and U=O bond strengths, as well as due to a better treatment of the hydrogen fluoride molecule (which is a product of the hydrolysis reaction) by this functional.

For the DFT methods presented in Table 7, we note a marked difference between hydrolysis reactions and any other reactions studied here with respect to the influence of different relativistic methods and basis sets on the reaction energies. For the latter, DFT methods with different basis sets and relativistic methods gave close values for the energies for a given functional. However, for the former the SC-ECP calculation in the B1 basis set yields results significantly different from the other methods (and much worse compared with the experiment). Moreover, the divergence is rising from reaction (13) to (14) to (15).

Privalov et al.[28] in their study of reactions (1), (14) and (15) with SCF, hybrid DFT and correlated wavefunction methods, found a very similar picture. They explained the results as a failure of all methods used in the treatment of the hydrolysis product, hydrogen fluoride. Consequently, they used another process (HF formation from $H_2$ and $F_2$) to calibrate the calculated values of their hydrolysis energies in order to obtain better agreement with the experimental enthalpies. We note that these authors used a relatively small basis set for the ligands. Indeed, changing the basis from B1 to the bigger B2 set in our SC-ECP calculations (Table 7) dramatically shifts the calculated DFT energies towards the values given by AE/L1 and ZORA/TZP methods and basis sets.

We note that for the AE-DZP case, although there is some increase in deviation from the experiment with increasing number of the hydrogen fluoride molecules on the right hand of the reaction equation, the magnitude is much less than the one of PBE0 with SC-ECP and the B1 basis set. Therefore, we conclude that the "standard" 6-31g* family basis sets for the ligands (which were part of the B1 set used by us) should not be used with DFT calculations. A good optimised Gaussian basis set, even of the rather modest DZP-quality as L1, is sufficient to obtain results with reasonable accuracy without resorting to a calibration procedure.

**Higher-order correlation method: CCSD(T) single-point energies**

As one might notice from the above discussion, the energies of our model reactions, as given by the AE-MP2 correlation method, are rather poor and inferior to the ones given by hybrid DFT—even within either the large L3 basis or the complete basis set extrapolation scheme. Therefore it would be interesting to check whether a higher wavefunction-based correlation method within the same single-reference, scalar four-component relativistic Scheme could perform better than MP2. We chose to test the coupled-cluster

  

method including singles, doubles, and perturbative triples (CCSD(T).[36,38] It is not possible at present, for various technical reasons, to optimize the geometries at this level of theory, nor is it feasible to use very extended bases such as L2 and L3. Thus, we chose to use single-point CCSD(T)/L1 calculations on MP2/L3 optimised geometries. Just as for the MP2/CBS calculations, the MP2/L2 frequencies were used. Resulting enthalpies for our test reactions (1) to (15) are provided in Table 9. In order to (rather crudely) estimate the effects of the basis set size on the calculated reaction energies, we have added the difference between the complete basis set MP2 values and the MP2/L1 values to the CCSD(T)/L1 energies. Resulting enthalpies are marked in the Table 9 as AE-CCSD(T)-"corrected". We realize that this simple correction is very crude, for the MP2 method is not variational and can both over- and underestimate the correlation energy; thus, the part which is recovered by the CBS approximation might be higher or lower for CCSD(T) than for MP2. Nonetheless, it gives us some idea in which direction extending the basis set for CCSD(T) calculations to L2, L3, and others would shift our reaction enthalpies.

One can see that the coupled-cluster method greatly improves all the reaction enthalpies for the dissociation reactions compared with MP2. Differences between them and the experiment are much lower especially for the U–F dissociation reactions. In general, the CCSD(T) results for dissociation enthalpies are close to the ones by hybrid DFT. For the hydrolysis reactions (13)–(15), the coupled cluster method gave better agreement with experiment than hybrid DFT, probably because of a better description of hydrogen fluoride. However, while improving the enthalpies of the conproportionation reactions (2) and (3) compared with MP2, CCSD(T) does overestimate the exothermicity of reaction (1) significantly. Indeed, taking reaction (1) out reduces the mean error from $-5.3$ to $-4.2$ kcal mol$^{-1}$ and the mean absolute error from 6.9 to 5.9 kcal mol$^{-1}$ (with similar changes for the corrected CCSD(T) numbers).

## Conclusion

Small uranium(IV, V, VI) oxofluorides were studied by using three different relativistic approximations: the scalar four component all-electron method, small-core effective core potentials and the zeroth-order regular approximation with GGA density functional theory. For the scalar four-component and small-core ECP methods, the hybrid DFT functional PBE0 was applied as well. Usage of a modern, new-generation quantum chemistry code such as Priroda allowed, for the first time, for comparison of these DFT results against relativistic scalar four component all-electron MP2 calculations within the complete basis set extrapolation approach. This approach ensures that there is no error cancellation on the basis set part, and therefore our AE-MP2 results reflect the characteristics of the MP2 method itself.

All three relativistic methods, as implemented in various codes (Priroda-AE, ADF-ZORA, Gaussian03-SC-ECP) give very similar results for geometries, frequencies and reaction enthalpies, provided that the same density functional and comparable quality basis set are used. This can be seen as a verification of these relativistic methods.

On the other hand, differences between the correlation methods tested are found to be significant. In some cases, different correlation methods lead to different uranium oxofluoride geometries. Analysis of charges and bond orders in the uranium complexes studied shows that pure GGA density functionals always predict more covalent bonding than hybrid functionals (and, likely, the MP2 method). Covalent bonds are known to be directional; moreover, for complexes of earlier transition-metal complexes it is known that an increase in covalent character of the σ (and in some cases π) metal-to-ligand bonding favours non-VSEPR structures.[73] This might be the case for the earlier actinide complexes as well. Thus, the fact that the GGA methods predicted a non-VSEPR $C_s$ structure for $UOF_4$ and lower F-U-F angles in the see-saw type molecule $UO_2F_2$, as well as higher symmetry for low-valent uranium complexes as $UOF_2$ might be the result of overestimated covalency of U=O and U−F bonds by these methods. Our results for $UOF_4$ are in agreement with previous ZORA GGA calculations of Kovacs and Konings.[31] However, we also tested two different relativistic approaches (AE four component and SC-ECP) as well as a range of GGA density functionals. Therefore we can conclude that these results are not artifacts of ZORA or the particular functional but are characteristic for GGA DFT method in general.

The geometries of the complexes studied were found to be influenced by the inverse *trans*-influence of the oxygen ligands. This is especially true for the uranium(VI) molecules. The ITI on geometries shows stronger for the more "ionic" results from hybrid DFT and MP2 calculations than for the GGA ones. For lower-valent complexes such as $UOF_2$, which have two unpaired electrons in the f orbitals at uranium resulting in near-degenerate electronic configurations, hybrid DFT and MP2 methods give lower symmetry geometries than GGAs due to Jahn–Teller distortion. Unexpectedly, for uranium trioxide, the MP2 method was found to give very different geometries for different basis sets (and relativistic methods as well; however it is unclear if the SC-ECP result—$C_{3v}$ symmetry for $UO_3$—is an effect of the basis set size or a consequence of the wrong nodal structure of ECP bases), while both GGA and hybrid DFT methods predicted a T-shaped "uranyl-oxide" structure in agreement with the experimentally IR-estimated symmetry in a solid noble gas matrix.

Bond lengths given by hybrid DFT are systematically shorter than the ones from pure GGA. The MP2 method, especially with the higher L2 and L3 basis sets, gave bonds even shorter than the hybrid PBE0. While there is not much experimental information on gas-phase geometries available (the only one we are aware of is the $UF_6$ case, for which the PBE0 geometry shows the best agreement), there is a well-known correlation between bond length and the corresponding vibrational frequency. However, for the U=O frequen-

  

cies, all the GGA functionals studied gave the closest agreement to experiment whereas PBE0 overestimated the values systematically. MP2 results for frequencies are not significantly better than hybrid DFT: moreover, they were not as uniform as for the latter.

The performance of the methods for the thermochemistry of uranium oxofluorides was tested on a set of homolytic fluorine and oxygen dissociation reactions as well as on the (non-isodesmic) hydrolysis and conproportionation reactions containing only closed-shell, uranium(VI) compounds. The qualitative picture for relative bond strengths for the former set was in agreement with the latter, which gives confidence in the single-reference, scalar relativistic methodology applied.

Hybrid DFT was found to be superior to GGA and MP2 for thermochemistry; considering that no spin-orbit and non-dynamic correlation effects were taken into account, PBE0 shows encouraging agreement with the available experiment, both qualitative and quantitative. This pattern holds not only for U−F bond dissociations, as was known from works of Batista, Hay and Martin,[19] but for U=O multiple bonds as well. The single-point CCSD(T) calculations give reaction enthalpies that are close to those from hybrid DFT, especially for dissociation reactions.

Pure GGA functionals were found to overestimate U−F as well as U=O bond dissociation energies compared with the experiment. Moreover, we found that the overestimation is not uniform but depends on the environment: bond energies in fluorine-rich complexes are overestimated stronger than in complexes with higher content of oxygen. Varying density functionals within the GGA approach does not lead to significant improvement of the calculated dissociation reaction enthalpies; from the functionals tested, OLYP results are slightly better than the others.

Although the MP2 method is sometimes still considered more reliable than hybrid DFTs, we found that its performance for thermochemistry was not as good. The method gives non-uniform errors comparable to those of the GGA methods, but in a different way: while bond energies in uranium fluorides were only slightly overestimated compared with the experiment and PBE0 calculations, both U−F and U=O energies in oxygen-containing uranium complexes were overestimated much stronger.

## Acknowledgements

The authors are grateful to D. N. Laikov for making his Priroda code available to us, for various suggestions as well as critical reading of the manuscript, and for performing the CCSD(T) calculations. The authors acknowledge financial support from the Natural Sciences and Engineering Research Council of Canada (NSERC) and from the University of Manitoba (start-up funds and University of Manitoba Research Grants Program). T.N.V. acknowledges additional financial support from Human Resources and Skills Development Canada through the Summer Career Placements program.

[1] W. Koch, M. C. Holthausen, *A Chemist's Guide to Density Functional Theory*, Wiley-VCH, New York, **2000**.
[2] M. Pepper, B. E. Bursten, *J. Am. Chem. Soc.* **1990**, *112*, 7803–7804.
[3] G. Schreckenbach, P. J. Hay, R. L. Martin, *J. Comput. Chem.* **1999**, *20*, 70–90.
[4] N. Kaltsoyannis, *Chem. Soc. Rev.* **2003**, *32*, 9–16.
[5] G. A. Shamov, G. Schreckenbach, *J. Phys. Chem. A* **2006**, *110*, 1207.
[6] I. R. Beattie, *Angew. Chem.* **1999**, *111*, 3494–3507; *Angew. Chem. Int. Ed.* **1999**, *38*, 3295–3306.
[7] X. F. Wang, L. Andrews, J. Li, B. E. Bursten, *Angew. Chem.* **2004**, *116*, 2608–2611; *Angew. Chem. Int. Ed.* **2004**, *43*, 2554–2557.
[8] D. L. Hildenbrand, K. H. Lau, *Pure Appl. Chem.* **1992**, *64*, 87–92.
[9] D. L. Hildenbrand, K. H. Lau, *J. Chem. Phys.* **1991**, *94*, 1420–1425.
[10] K. H. Lau, D. L. Hildenbrand, *J. Chem. Phys.* **1987**, *86*, 2949–2954.
[11] K. H. Lau, R. D. Brittain, D. L. Hildenbrand, *J. Phys. Chem.* **1985**, *89*, 4369–4373.
[12] K. H. Lau, D. L. Hildenbrand, *J. Chem. Phys.* **1984**, *80*, 1312–1317.
[13] L. N. Gorokhov, V. K. Smirnov, Y. S. Khodeev, *Zhurnal Fiz. Khimii* **1984**, *58*, 1603–1609.
[14] B. B. Ebbinghaus, O. H. Krikorian, D. L. Fleming, "Thermodynamic Study of $UO_3$(g), $UO_2(OH)_2$(g), $UO_2Cl_2$(g), and $UO_2F_2$(g) UCLR-ID-150979, Lawrence Livermore National Laboratory, US Department of Energy, **2002**.
[15] M. F. Zhou, L. Andrews, N. Ismail, C. Marsden, *J. Phys. Chem. A* **2000**, *104*, 5495–5502.
[16] D. W. Green, G. T. Reedy, S. D. Gabelnick, *J. Chem. Phys.* **1980**, *73*, 4207–4216.
[17] G. Schreckenbach, *Inorg. Chem.* **2000**, *39*, 1265–1274.
[18] E. R. Batista, R. L. Martin, P. J. Hay, *J. Chem. Phys.* **2004**, *121*, 11104–11111.
[19] E. R. Batista, R. L. Martin, P. J. Hay, J. E. Peralta, G. E. Scuseria, *J. Chem. Phys.* **2004**, *121*, 2144–2150.
[20] M. Douglas, N. M. Kroll, *Ann. Phys.* **1974**, *82*, 89.
[21] A. Wolf, M. Reiher, B. A. Hess, *J. Chem. Phys.* **2002**, *117*, 9215–9226.
[22] Q. Wang, R. M. Pitzer, *J. Phys. Chem. A* **2001**, *105*, 8370–8375.
[23] M. Straka, K. G. Dyall, P. Pyykkö, *Theor. Chem. Acc.* **2001**, *106*, 393–403.
[24] W. Küchle, M. Dolg, H. Stoll, H. Preuss, *J. Chem. Phys.* **1994**, *100*, 7535–7542.
[25] Y. A. Teterin, V. A. Terehov, M. V. Ryzhkov, I. O. Utkin, K. E. Ivanov, A. Y. Teterin, A. S. Nikitin, *J. Electron Spectrosc. Relat. Phenom.* **2001**, *114*, 915–923.
[26] C. Clavaguera-Sarrio, S. Hoyau, N. Ismail, C. J. Marsden, *J. Phys. Chem. A* **2003**, *107*, 4515–4525.
[27] P. Pyykkö, J. Li, N. Runeberg, *J. Phys. Chem.* **1994**, *98*, 4809–4813.
[28] T. Privalov, B. Schimmelpfennig, U. Wahlgren, I. Grenthe, *J. Phys. Chem. A* **2002**, *106*, 11277–11282.
[29] B. Schimmelpfennig, T. Privalov, U. Wahlgren, I. Grenthe, *J. Phys. Chem. A* **2003**, *107*, 9705–9711.
[30] A. Kovacs, R. J. M. Konings, *THEOCHEM* **2004**, *684*, 35–42.
[31] A. Kovacs, R. J. M. Konings, *Chemphyschem* **2006**, *7*, 455–462.
[32] C. Clavaguera-Sarrio, V. Vallet, D. Maynau, C. J. Marsden, *J. Chem. Phys.* **2004**, *121*, 5312–5321.
[33] L. V. Moskaleva, A. V. Matveev, S. Krüger, N. Rösch, *Chem. Eur. J.* **2005**, *11*, 629–634.
[34] V. Vetere, P. Maldivi, C. Adamo, *J. Comput. Chem.* **2003**, *24*, 850–858.
[35] C. Clavaguera-Sarrio, N. Ismail, C. J. Marsden, D. Begue, C. Pouchan, *Chem. Phys.* **2004**, *302*, 1–11.
[36] D. N. Laikov, Personal Communication, **2006**.
[37] C. Møller, M. S. Plesset, *Phys. Rev.* **1934**, *46*, 618.
[38] K. Raghavachari, G. W. Trucks, J. A. Pople, M. Head-Gordon, *Chem. Phys. Lett.* **1989**, *157*, 479–483.
[39] D. N. Laikov, *Chem. Phys. Lett.* **1997**, *281*, 151–156.
[40] D. N. Laikov, DFT2000 Conference, Menton (France) **2000**.
[41] D. N. Laikov, Priroda code, **2006**.
[42] K. G. Dyall, *J. Chem. Phys.* **1994**, *100*, 2118–2127.

  

[43] D. N. Laikov, *Chem. Phys. Lett.* **2005**, *416*, 116–120.
[44] D. N. Laikov, unpublished results.
[45] B. I. Dunlap, J. W. D. Connolly, J. R. Sabin, *J. Chem. Phys.* **1979**, *71*, 3396–3402.
[46] E. van Lenthe, E. J. Baerends, J. G. Snijders, *J. Chem. Phys.* **1993**, *99*, 4597–4610.
[47] E. van Lenthe, E. J. Baerends, J. G. Snijders, *J. Chem. Phys.* **1994**, *101*, 9783–9792.
[48] E. van Lenthe, A. Ehlers, E. J. Baerends, *J. Chem. Phys.* **1999**, *110*, 8943–8953.
[49] G. te Velde, F. M. Bickelhaupt, E. J. Baerends, C. Fonseca Guerra, S. J. A. van Gisbergen, J. G. Snijders, T. Ziegler, *J. Comput. Chem.* **2001**, *22*, 931–967.
[50] C. Fonseca Guerra, O. Visser, J. G. Snijders, G. te Velde, E. J. Baerends in *Methods and Techniques in Computational Chemistry METECC-95* (Eds.: E. Clementi, C. Corongiu), STEF, Cagliari (Italy), **1995**, pp. 305–395.
[51] ADF 2004.01, E. J. Baerends, A. J. A., A. Bérces, C. Bo, P. M. Boerrigter, L. Cavallo, D. P. Chong, L. Deng, R. M. Dickson, D. E. Ellis, L. Fan, T. H. Fischer, C. Fonseca Guerra, S. J. A. van Gisbergen, J. A. Groeneveld, O. V. Gritsenko, M. Grüning, F. E. Harris, P. van den Hoek, H. Jacobsen, G. van Kessel, F. Koostra, E. van Lenthe, D. A. McCormack, V. P. Osinga, S. Patchkovskii, P. H. T. Philipsen, D. Post, C. C. Pye, W. Ravenek, P. Ros, P. R. T. Schipper, G. Schreckenbach, J. G. Snijders, M. Sola, M. Swart, D. Swerhone, G. te Velde, P. Vernooijs, L. Versluis, O. Visser, E. van Wezenbeek, G. Wiesenekker, S. K. Wolff, T. K. Woo, T. Ziegler, Scientific Computing and Modelling, Theoretical Chemistry, Vrije Universiteit, Amsterdam (The Netherlands), **2004**.
[52] Gaussian 03, M. J. Frisch, G. W. Trucks, H. B. Schlegel, G. E. Scuseria, M. A. Robb, J. R. Cheeseman, J. A. Montgomery, T. Vreven, K. N. Kudin, J. C. Burant, J. M. Millam, S. S. Iyengar, J. Tomasi, V. Barone, B. Mennucci, M. Cossi, G. Scalmani, N. Rega, G. A. Petersson, H. Nakatsuji, M. Hada, M. Ehara, K. Toyota, R. Fukuda, J. Hasegawa, M. Ishida, T. Nakajima, Y. Honda, O. Kitao, H. Nakai, M. Klene, X. Li, J. E. Knox, H. P. Hratchian, J. B. Cross, V. Bakken, C. Adamo, J. Jaramillo, R. Gomperts, R. E. Stratmann, O. Yazyev, A. J. Austin, R. Cammi, C. Pomelli, J. W. Ochterski, P. Y. Ayala, K. Morokuma, G. A. Voth, P. Salvador, J. J. Dannenberg, V. G. Zakrzewski, S. Dapprich, A. D. Daniels, M. C. Strain, O. Farkas, D. K. Malick, A. D. Rabuck, K. Raghavachari, J. B. Foresman, J. V. Ortiz, Q. Cui, A. G. Baboul, S. Clifford, J. Cioslowski, B. B. Stefanov, G. Liu, A. Liashenko, P. Piskorz, I. Komaromi, R. L. Martin, D. J. Fox, T. Keith, M. A. Al-Laham, C. Y. Peng, A. Nanayakkara, M. Challacombe, P. M. W. Gill, B. Johnson, W. Chen, M. W. Wong, C. Gonzalez, J. A. Pople, Gaussian, Inc., Wallingford CT, **2004**.
[53] http://www.emsl.pnl.gov/forms/basisform.html Basis sets were obtained from the Extensible Computational Chemistry Environment Basis Set Database, Version 02/25/04, as developed and distributed by the Molecular Science Computing Facility, Environmental and Molecular Sciences Laboratory which is part of the Pacific Northwest Laboratory, P.O. Box 999, Richland, Washington 99352 (USA), and funded by the US Department of Energy. The Pacific Northwest Laboratory is a multi-program laboratory operated by Battelle Memorial Institute for the US Department of Energy under contract DE-AC06-76RLO 1830. Contact Karen Schuchardt for further information.
[54] R. A. Kendall, T. H. Dunning, R. J. Harrison, *J. Chem. Phys.* **1992**, *96*, 6796–6806.
[55] J. P. Perdew, K. Burke, M. Ernzerhof, *Phys. Rev. Lett.* **1996**, *77*, 3865–3868.
[56] M. Ernzerhof, G. E. Scuseria, *J. Chem. Phys.* **1999**, *110*, 5029–5036.
[57] C. Adamo, V. Barone, *J. Chem. Phys.* **1999**, *110*, 6158–6170.
[58] V. Vetere, C. Adamo, P. Maldivi, *Chem. Phys. Lett.* **2000**, *325*, 99–105.
[59] C. Adamo, V. Barone, *J. Chem. Phys.* **2002**, *116*, 5933–5940.
[60] A. D. Becke, *Phys. Rev. A* **1988**, *38*, 3098–3100.
[61] C. Lee, W. Yang, R. G. Parr, *Phys. Rev. B* **1988**, *37*, 785.
[62] N. C. Handy, A. J. Cohen, *Mol. Phys.* **2001**, *99*, 403–412.
[63] I. Mayer, Simple theorems, proofs, and derivations in quantum chemistry, Kluwer Academic/Plenum Publishers, New York, **2003**, p. 337.
[64] F. L. Hirshfeld, *Theor. Chim. Acta* **1977**, *44*, 129–138.
[65] D. W. Green, *Int. J. Thermophys.* **1980**, *1*, 61–71.
[66] H. M. Seip, *Acta Chem. Scand.* **1966**, *20*, 2698–2710.
[67] M. Kimura, V. Schomaker, D. W. Smith, B. Weinstock, *J. Chem. Phys.* **1968**, *48*, 4001–4012.
[68] M. Straka, M. Patzschke, P. Pyykkö, *Theor. Chem. Acc.* **2003**, *109*, 332–340.
[69] R. T. Paine, R. R. Ryan, L. B. Asprey, *Inorg. Chem.* **1975**, *14*, 1113–1117.
[70] R. Boughon, J. Fawcett, J. H. Holloway, D. R. Russell, *J. Chem. Soc. Dalton Trans.* **1979**, 1881–1885.
[71] R. G. Denning, *Struct. Bonding (Berlin)* **1992**, *79*, 215–276.
[72] E. O'Grady, N. Kaltsoyannis, *J. Chem. Soc. Dalton Trans.* **2002**, 1233–1239.
[73] M. Kaupp, *Angew. Chem.* **2001**, *113*, 3642–3677; *Angew. Chem. Int. Ed.* **2001**, *40*, 3534–3565.

Received: August 30, 2006
Published online: March 20, 2007

  